EFFECTS OF MESSENGER MOLECULE DEGRADATION IN MOLECULAR COMMUNICATION VIA DIFFUSION

by

Akif Cem Heren

B.S., Computer Engineering, Bogazici University, 2012

Submitted to the Institute for Graduate Studies in
Science and Engineering in partial fulfillment of
the requirements for the degree of
Master of Science

Graduate Program in Computer Engineering

Boğaziçi University

2014

EFFECTS OF MESSENGER MOLECULE DEGRADATION IN MOLECULAR COMMUNICATION VIA DIFFUSION

APPROVED BY:

Assoc. Prof. Tuna Tugcu ..... (Thesis Supervisor)

Prof. Cem Ersoy .....

Assist. Prof. Ali Emre Pusane .....

DATE OF APPROVAL: 15.08.2014

ACKNOWLEDGEMENTS

First of all, I would like to thank to my supervisor Assoc. Prof. Tuna Tugcu for his endless support and encouragement dating back to my undergraduate years. Along with Professor Tugcu, the nanonetworking research group have given me tremendous insight which helped me to build the clear path that lead to this thesis. In this regard I would like to thank -beginning with now former members of the group- H. Birkan Yılmaz, M. Şükrü Kuran, Ali Akkaya, Gaye Genç, and Fadik Kılıçlı for their invaluable accompaniment.

Second, I would like to thank all my family, beginning with my brother Hasan Alp Heren and my mother Zerrin Heren, who always been there for me with their love and support.

Finally, I want to thank my friends, Mert Alioğlu, Özgün Yücetürk, Çiğdem Koçberber, Mustafa Tuğrul Özşahin, and of most of all, M. Sevgi Şen for their patience, ideas, comments, discussions, and support during the past two years in which this thesis is created.

This thesis is partly supported by State Planning Organization (DPT) of Republic of Turkey under the project TAM with the project number 2007K120610, Bogazici University Research Fund (BAP) under grant number 7436, and by Scientific and Technical Research Council of Turkey (TUBITAK) under Grant number 112E011.

ABSTRACT

EFFECTS OF MESSENGER MOLECULE DEGRADATION IN MOLECULAR COMMUNICATION VIA DIFFUSION

Nanonetworking is a promising new paradigm that focuses on communication between nanoscale machines. In the nanonetworking literature, many solutions have been suggested to enable the information transfer between nano-machines. Among these solutions, we focus on molecular communication via diffusion which constitutes a basis for many types of molecular communication. Specifically, we start with the analytical model of 3-D absorbing receiver under messenger molecule degradation and show that our formulations are in agreement with the simulation results. Next, we identify the effects of degradation in signal characteristics such as pulse peak time and pulse amplitude, and we analytically show how degradation is used for signal shaping in molecular communication via diffusion. Here, we also compare communication under degradation with the case of no degradation and electromagnetic communication in terms of channel characteristics. Lastly, we evaluate the performance of the degradation system for different choices of degradation rates. Here, we assess the system performance according to traditional network metrics such as the level of inter-symbol interference, detection performance, bit error rate, and data rate. Our results indicate that introducing degradation significantly improves the system performance. For a given distance, increasing degradation rate also increases the system performance in terms of all metrics mentioned above up to a peak performance point. However, after the peak point, degradation becomes too fast and causes most of the molecules to degrade before reaching the receiver, which in turn deteriorates the system performance.

ÖZET

HABERLEŞME MOLEKÜLÜ YIKIMIMIN DİFÜZYON İLE HABERLEŞME ÜZERİNE ETKİLERİ

Nanoağlar nanometre ölçüsündeki makineler arası iletişimin gerçekleştirilmesi adına umut vaat eden yeni bir kavramdır. Nanoağlar literatüründe önerilen çözümler arasından; bu tezde, birçok moleküler haberleşme türüne temel oluşturan Moleküler Difüzyon ile Haberleşme sistemine odaklanılmaktadır. Tez içerisinde, ilk olarak, haberleşme molekülü yıkımı olan kanallarda soğurma özelliği olan alıcıların 3-B küre şeklinde analitik olarak modellenmesi ele alınmakta, formülasyon ve simülasyon arasındaki uyuşmalar gösterilmektedir. İkinci olarak, sinyal zirve noktası zamanı ve sinyal zirve noktası enliği gibi metrikler kullanılarak molekül yıkımının sinyal karakteristiklerine olan etkileri analitik olarak gösterilmektedir. Burada, haberleşme molekülü yıkımına tabi olan sistem, yıkıma tabi olmayan sistem ve elektromanyetik iletişim kanalı belirtilen karakteristikler açısından karşılaştırılmaktadır. Son olarak, farklı molekül yıkımı hızlarına göre sistem performansı değerlendirilmektedir. Burada, sistem performansı semboller arası girişim, algılama performansı, bit hata oranı ve veri hızı gibi geleneksel ağ metrikleri ile değerlendirilmektetir. Sonuçlar, molekül yıkımı kullanılan sisemlerin doğru koşullar altında kayda değer performans artışı sağladığını göstermektedir. Belirli bir iletişim uzaklığı için, molekül yıkım hızını artırmak sistem performansını bahsi geçen tüm metriklerde bir tepe noktasına kadar artırmaktadır. Ancak, bu noktadan sonra, hızlı molekül yıkımının çoğu molekülün alıcıya ulaşamadan yıkılmasına ve sonuç olarak sistem başarımının düşmesine sepep olduğu gözlenmektedir.

TABLE OF CONTENTS

LIST OF FIGURES

LIST OF TABLES

LIST OF SYMBOLS

$\mathcal{B}$	Binomial Distribution
C_0	Initial concentration under degradation
$C(t)$	Concentration as a function of time under degradation
d	Distance of the transmitter to the surface of receiver
D	Diffusion coefficient
$\mathcal{D}(.)$	Demodulation function for the received molecules
$\mathbb{E}[t_{\text{peak}}]$	Expected pulse peak point
$\mathbb{E}[t_{\text{peak}}\|\lambda]$	Expected pulse peak point given degradation with rate λ
$\mathbb{E}[n_{\text{peak}}]$	Expected fraction of peak pulse amplitude
$\mathbb{E}[n_{\text{peak}}\|\lambda]$	Expected fraction of peak pulse amplitude given degradation with rate λ
$f_A(t)$	Probability distribution function of event A
$F(t)$	Cumulative distribution function
$\bar{F}(t)$	Complementary cumulative distribution function
$h(t)$	Channel response function
$h(\Omega_r, t\|r_0)$	Channel response function corresponding to an absorbing receiver surface Ω_r, time t given the initial burst occurring at r_0
$h(\Omega_r, \lambda, t\|r_0)$	Channel response function corresponding to an absorbing receiver surface Ω_r, time t given the initial burst occurring at r_0, and the rate of degradation λ
$\mathcal{K}_u$	Time independent coefficient on $\mathcal{U}(k, t\|r_0)$
$\mathcal{K}_v$	Time independent coefficient on $\mathcal{V}(r, s\|r_0)$
l_i	Initial coordinate point of a rectangular prism in a given dimension
l_f	Final coordinate point of a rectangular prism in a given dimension
$\mathcal{N}$	Gaussian Distribution
$N_{\text{Tx}}^{r_0}$	Number of released molecules on the initial burst
$N_{\text{Rx}}^{\Omega_r}(0, t)$	Number of received molecules between [0, t)

N_0	Number of molecules released to represent a bit-0
N_1	Number of molecules released to represent a bit-1
$p(d,t)$	Probability density function of molecule concentration at distance d and time t
$p(r,t\|r_0)$	Probability density function of molecule concentration at r distance and t time, given the initial burst of molecules occurred at r_0
$\mathcal{P}(r,s\|r_0)$	Laplace transform of $p(r,t\|r_0)$
$P_B(T>t)$	Probability of event B happening later then time t
$\mathcal{P}$	Poisson Distribution
$Pc_1(\tau,\lambda,t_i\|s_i=1)$	Probability of correct detection of a bit-1 in ith symbol duration with a demodulation threshold τ and degradation coefficient λ
$Pc_0(\tau,\lambda,t_i\|s_i=0)$	Probability of correct detection of a bit-0 in ith symbol duration with a demodulation threshold τ and degradation coefficient λ
$Pc_1(\tau,\lambda)$	Probability of correct detection of a bit-1 in the channel with a demodulation threshold τ and degradation coefficient λ
$Pc_0(\tau,\lambda)$	Probability of correct detection of a bit-0 in the channel with a demodulation threshold τ and degradation coefficient λ
Pe	Overall probability of error
Pe_1	Probability of erroneous detection of bit-1
Pe_0	Probability of erroneous detection of bit-0
P_f	Probability of false alarm
P_d	Probability of correct detection
r_0	Distance of the transmitter to the center of receiver
r_r	Radius of the spherical receiver
$r(\Omega_r,\lambda,t\|r_0)$	Ratio of molecules that remain unreceived for one burst of molecules at time t
s_i	The bit value of the ith bit
t_s	Symbol duration
t_k	The point in time where the kth symbol duration ends

$u(r,t\|r_0)$	Probability density function obeying first half of boundary conditions imposed on a spherical absorber
$\mathcal{U}(k,t\|r_0)$	Fourier transform of $u(r,t\|r_0)$
$\mathcal{U}(r,s\|r_0)$	Laplace transform of $u(r,t\|r_0)$
$v(r,t\|r_0)$	Probability density function obeying first second of boundary conditions imposed on a spherical absorber
$\mathcal{V}(r,s\|r_0)$	Laplace transform of $v(r,t\|r_0)$
$w(\Omega_r,t\|r_0)$	Received fraction of the molecules by the receiver (Ω_r) until time t
$w(\Omega_r,\lambda\|r_0)$	Probability of getting absorbed before getting degraded for a messenger molecule
$w(\Omega_r,\lambda,t\|r_0)$	Received fraction of the molecules by the receiver (Ω_r) until time t with degradation of rate λ
$w_c(\Omega_r,t_1,t_2\|r_0)$	Channel response between times t_1 and t_2
$w_c(\Omega_r,\lambda,t_1,t_2\|r_0)$	Channel response between times t_1 and t_2 with degradation of rate λ
$w_s(\Omega_r,\lambda,t_i\|r_0)$	The sum of all channel responses that represent bit-1 until the ith symbol and the current symbol itself
Y_i	Number of molecules arriving at the receiver in ith symbol duration as a binomial random variable
Y_i^m	The number of received molecules in ith symbol duration due to emission at the mth symbol duration
α	Rate of reaction in the absorptive boundary of the receiver
$\delta(.)$	Delta-dirac function
Δt	Simulation step size
λ	Rate of degradation
$\Lambda_{1/2}$	Half-life of the degrading molecule
ξ	Infinitesimal time frame
τ	Demodulation threshold
Ω_r	Receiver surface
∇	Laplacian operator

LIST OF ACRONYMS/ABBREVIATIONS

3-D	Three dimensional
ACh	Acetylcholine
AChE	Acetylcholinesterase
AM	Amplitude modulation
ATP	Adenosine-tri-phosphate
BER	Bit error rate
ccdf	Complementary cumulative distribution function
CNT	Carbon nano-tube
CSK	Concentration shift keying
DNA	Deoxyribonucleic acid
EDR	Estimated data rate
ES	Embryonic stem
EM	Electromagnetic
FRET	Förster Resonance energy transfer
IP_3	Inositol-tri-phosphate
ISI	Inter symbol interference
MCvD	Molecular communication via diffusion
MFSK	Molecular frequency shift keying
MM	Messenger molecule
MoSK	Molecular shift keying
PLC	Phospholipase C
rDNA	Recombinant DNA
ROC	Receiver operating characteristics
THz	Tera hertz

1. INTRODUCTION

1.1. Prologue

It would not be the farthest assessment from reality if we claimed computer scientists look up to the nature for inspiration to find a solution to a problem that is created by a process altogether inspired by nature in an earlier instance. Today we are getting our inspiration from the nature about the collective harmony of -very- small scale components (molecules, cells), which creates a variety of considerably large scale effects on our lives. This process leaves us standing at the verge of the birth of a new paradigm, that is both familiar and alien to us, concerning the set of self operating matter of size in close proximity to one-billionth of a meter.

Scientist has long started *the journey to the bottom*, investigating vast possibilities offered by nanotechnology. We, computer scientists, -never like to be the last arriving- expectedly started looking for ways to have these rather small machinery to talk to each other. Inspired from nature and our past experiences, we are modeling and designing ways of communication that will be efficient in our traditional measures and bio-friendly in the levels we have never done before. We are ready to keep our hopes high about the future we herein aspire to design.

1.2. Sizing down to nanometer scale

1.2.1. Nanomachines

Nanomachines are self operating machines in the sizes of few nanometers. They are envisioned to be placed in extreme environments where their macro scale counterparts are not able to exist such as inside the bloodstream or maybe a bottle of water. In the literature, nanomachines, following their extremely small sizes, are mostly considered to operate in vivo for medical purposes.[1]

[1] In vivo: Inside a living organism

The utilization of nanomachines in medicine may lead to a great increase in patient well-being. By nature, these nanomachines are expected to be almost noninvasive when they are performing medical tasks. As a profound example, we can one day expect a group of nanomachines, injected into the bloodstream, to locate and kill a tumor applying only the required medicine to the specific location of the tumor in the body, as opposed to a tedious, much more coarse, chemotherapy process. In the literature, examples of molecular sensing and drug delivery have been promised by a variety of studies [1, 2]. Among those examples, achieving drug delivery to a solid tumor by using nanoparticles given by a dose of vaccination [3] and achieving spatiotemporal pH changes inside living cells using DNA nanomachines [4], stand tall.

1.2.2. Nanonetworks

In order to enhance the potential of nanomachines, the most straightforward way is to connect them and enable them to act together to achieve a superior task. The nanonetworking field is built around the promise that individual nanomachines will be too simple to make an impact on the macro scale, and interaction among these machines will be a necessity. With the establishment of nanonetworks, it is possible to imagine capable networks of nanomachines working in coordination.

In the literature, there are several approaches in which researchers envision to build nanonetworks. At first, methods from traditional communication have been applied in the nanoscale. Later, different approaches similar to the communication techniques that are employed in the nature have been favored for their higher compatibility with the in vivo systems and medical applications. We elaborate on all of these techniques in Chapter 2.

One of the most important aspects of molecular communication is messenger molecule degradation. Although in nature, it is abundantly dominant to have degradation in a molecular communication scenario (ex: synaptic communication, pheromone signaling), it is mostly overlooked in the nanonetworking literature. Accurate modeling of the receiver dynamics and clarification of the effects of messenger molecule

degradation are yet to be studied.

1.3. Contribution of this thesis

The main contributions of this thesis are articulated below:

- *Channel characteristics for the absorbing receiver*: To the best of our knowledge, the nanonetworking literature has extensively used approximate methods to model the nano-receptor. In this thesis, we utilize channel response of the more realistic case of an absorbing spherical receiver in 3-D to formulate accurate channel characteristics.
- *Channel response for the exponential degradation*: The nanonetworking literature also neglects the effects of messenger molecule degradation. For the first time in the literature, the channel response for absorbing spherical (3-D) receiver under exponential molecular degradation is derived in this thesis.
- *Channel characteristics for the exponential degradation*: We formulate the channel characteristics for the degradation case and compare them with the non-degradation case, considering the more realistic case of the 3-D absorbing spherical receiver.
- *Performance evaluation of the use of messenger molecule degradation in molecular communication*: We show the effects of messenger molecule degradation through analytical results we derive, where we evaluate the system performance under the degradation scenario with various metrics; receiver operating characteristic (ROC), bit error rate (BER), and expected data rate (EDR).

1.4. Outline

In this thesis, we focus on the effect of degradation in one of the most important nano-communication methods found in the nanonetworking literature. First, in Chapter 2, we give the relevant background information regarding various types of nano-scale communication, with extensive focus on communication via diffusion. In Chapter 3, we present the derivations of the channel response functions for the cases

with and without degradation, in the presence of a 3-D absorbing spherical receiver. In Chapter 4, we articulate the effects of degradation on channel characteristics and model the arrival of molecules. Moreover, in Chapter 5, we show the evaluation of system performance under various degradation scenarios and present the improvements that can be achieved by enabling messenger molecule degradation. Finally, with Chapter 6, we conclude the thesis.

2. BACKGROUND INFORMATION

In this chapter, we elaborate on the topics necessary for a thorough comprehension of the work presented in this thesis. We first give a walkthrough of the various communication techniques found in the nanonetworking literature. Next, we give a short genetic engineering perspective on creating bio-nanomachines. Lastly, we present a detailed overview on molecular communication via diffusion.

2.1. Types of Nano-scale Communication

2.1.1. Electromagnetic Communication

In [5], Jornet *et al.* claim that a nano-dipole antenna based on carbon nanotubes (CNTs) is able to generate electromagnetic signals in the band 0.1 - 10.0 THz. Moreover, in a following work, Jornet *et al.* develop a channel model and calculate channel capacity of this short range electromagnetic communication [6]. In the latter work, the authors show that the communication is heavily influenced by a new type of noise, namely molecular absorption noise. This noise causes significant path loss and only allows communication in very short distances. Electromagnetic communication is also considered inviable due to its high energy consumption. Lastly, in terms of energy, bit rate and bio-compatibility diffusion based communication systems are superior to the electromagnetic (EM) communication systems.

2.1.2. Förster Resonance Energy Transfer Based Communication

Förster Resonance Energy Transfer (FRET) is a non-radiative energy transfer method occurring between two fluorescent molecules via the exchange of excited states, i.e., excitons. FRET based nano-communication has first been studied in [7, 8] where the authors consider and model the communication channel between a donor fluorophore as the transmitter and an acceptor as the receiver nanomachine, where a single exciton is interchanged.

Later in [9], Kuscu *et al.* consider a longer range FRET based communication where multiple excitons are exchanged between transmitter and the receiver machines with the help of relay nodes that are also fluorophores. Lastly, in [10], the authors investigate a system of mobile fluorophores acting as sensor and actor nodes and study the system performance under the mobile scenario.

2.1.3. Calcium Signaling

Calcium signaling is a form of molecular communication which works based on the fluctuations of cytoplasmic concentration of the Calcium ion (Ca^{2+}). In the nature a wide variety of cell types utilize calcium signaling to propagate information. For example, legumes encode the type of root infection information, whether it is caused by fungi or bacteria, to the oscillation dynamics (chaoticity) [11]. Moreover, in [12], Höfer *et al.* argue that some information is conveyed with calcium oscillations to distant parts of the brain, where a thorough model of the travel of the oscillations through the astrocites is presented. The abundant existence of calcium signaling in the nature makes it a strong candidate for nano-communication.

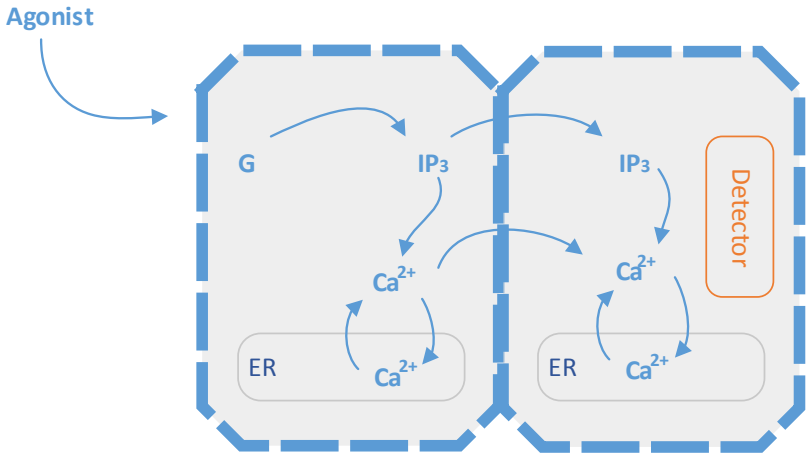

Figure 2.1. Calcium signaling in two consecutive cells.

In Figure 2.1, we depict the creation and propagation of a calcium oscillation in a two-cell grid. As described in [12], a calcium oscillation is initiated by an external agonist (this is the input signal for our purposes) acting on G-protein coupled receptors, which enable the release of Phospholipase C-beta (PLC_β) molecules. The

increase in PLC_β concentration triggers the release of inositol-tri-phosphate (IP_3) second messenger molecules, which ultimately causes a rapid discharge of Ca^{2+} from the sarcoplasmic reticulum (SERCA) resulting in elevated calcium concentration in the cytoplasm of the first cell. Later, diffusion of IP_3 molecules to the neighboring cells triggers the same action in those cells, again resulting in an elevated level of Ca^{2+} in the second cell. Meanwhile, the Calcium ions released in the first cell start being absorbed by the SERCA again, dropping the Ca^{2+} concentration in the first cell. The signal is propagated on the wave-like oscillation of the calcium ion concentration throughout the cell array.

From the nanonetworking perspective, in [13], Kuran *et al.* discuss various properties of inter-cellular calcium waves (oscillations). The authors argue that the existing infrastructure in the in-vivo systems can be used for the deployment of new applications. Moreover, the capability of inducing group behavior enables calcium signaling to be used to coordinate clusters of nanomachines. In [14], Nakano *et al.* consider a relay channel using calcium signaling for which they derive the communication capacity. Lastly, [15] defines the range of communication for calcium signaling as hundreds of micrometers, arguing that relatively longer distance communication can be achieved through calcium signals.

2.1.4. Communication via Molecular Motors

Molecular motors are used to carry various loads within the cell. These motors move along microtubules that are part of the cytoskeleton through which the cell maintains its rigid structure. Since the cytoskeleton covers a major portion of the cell, point-to-point communication is possible using the microtubule array.

In the literature, communication via molecular motors is often considered analogous to wired communication since the load can only travel between predetermined locations. In [16], Moore *et al.* propose a molecular motor based communication scheme where the microtubules are utilized as the tracks for the molecular motors. Moreover, in [17], Agarwal *et al.* consider an engineered surface where fixed molecular motors are

utilized as conveyor belts. In this model, microtubules are used as molecular shuttles upon which the load is assembled. In this methodology, the path of the shuttle can be controlled by various external factors, some of which are using specific surface topography, using electric or magnetic fields, or manipulating ATP concentration [17, 18].

2.1.5. Pheromone signaling

Pheromones are known as signaling molecules used for relatively long range communication in the nature, mostly between the members of a species. In nanonetworking one of the chief issues is to convey the information gathered in the nano-scale to the macro-scale, or to give supervised directions to a group of nanomachines through a form of signaling. Pheromone signaling has first been articulated in [19], in the nanonetworking perspective, as a means of long range communication that can be utilized in bio-inspired nanomachines.

Aside from nanonetworking the literature, robotics literature has studied pheromones in order to enable communication between robots where other means of communication is harder or less efficient to achieve. In [20], the authors achieve bi-directional communication between robot pairs and control the group using pheromones. Advantages for pheromone signaling include invisibility, immunity to electromagnetic interference, and robustness against communication barriers such as walls or doors. Disadvantages include high unpredictability, low bit rate, and limited sensor sensitivity.

2.1.6. Molecular Communication via Diffusion

Molecular communication via diffusion is the communication paradigm in which the information is carried through the propagation of messenger molecules by means of diffusion from the transmitter nanomachine to the receiver nanomachine. Most of the bio-inspired communication methods work based on MCvD; therefore, in the literature MCvD is extensively studied. A thorough overview is presented in Section 2.3.

2.2. Engineering the Cell

When a cell is considered as a nano-machine, the DNA is analogous to the source code of a program in execution. However, DNA not only controls the behavior of the system in terms of input and output, but it also regulates the physical properties of the machine such as growth, structure, or death. All cells in the nature, therefore, possess the right DNA sequence, which gives the cell the ability to perpetuate a self-sufficient life or perform its duties as a part of a larger organism in order to survive.

In genetics, scientists have found ways to modify the DNA sequences in order to alter or control the abilities and interactions of the cell. Most of these alterations are towards a new treatment for a disease or to gain a deeper understanding of a biologic entity that has yet to be fully comprehended. In the remainder of this section, we elaborate on some of the methods for altering cell behavior, not only from a perspective of understanding the underlying mechanisms but also from an engineering perspective of future construction of nano-machines.

2.2.1. Methods of Gene Transfer

The altered DNA, which is called recombinant DNA (rDNA) in the biology literature, is needed to be delivered to the host cell, which will act as an enabling body for the rDNA. Here, we elaborate on methods in biology literature for the transfer of the rDNA to the host cell [21].

Transfection. Transfection is a method initially tested in viral DNAs, where the new DNA molecule is directly embedded into the cells, via micro injection, transfer via lipid vesicles, etc. Transfection is characterized as a direct method where the injected DNA is taken up by most of the cells. However, in very few of the host cells ($\sim 1\%$) it becomes the part of the regular DNA of the cell, where it is duplicated similar to the older DNA and propagated to the upcoming generations. The reactive cells are then extracted and multiplied with the help of a selectable marker hidden in the new DNA

segment, such as resistance to a growth inhibiting drug.[2]

Transfer via viral vectors. As the name suggests, this methodology utilizes various kinds of viruses as the transport vehicle of the new DNA into the host cell. Viruses have been evolving for millions of years to learn how to penetrate and invade their target cell. Therefore, loading a virus with the desired new DNA, whilst enabling it to invade the target cell enables the virus to copy itself to the host cell's DNA. This operation creates a cell with the desired functionality while keeping the older DNA in the cell which enabled core functionalities such as reproduction or growth. Dating back to 1972 [22], biologists have utilized various virus types (adenoviral, retroviral/lentiviral, adeno-associated viral, herpesviral vectors) in gene therapy, while new methodologies such as hybrid vectors are being developed to elicit their shortcomings such as limited load capacity (that is DNA) and toxicity [23].

Direct injection to the germ line. This method requires direct microinjection of the cloned DNA to the fertilized egg of the multicellular organism. Direct injection enables the integration of the new DNA into all cells of the new born animal, allowing the creation of generations of new animals with differentiated genes.

Transfer via Embryonic Stem (ES) cells. In this method, the ES cells of early embryos are collected and their DNA sequence is altered in vitro. Then, these cells are reintroduced into the embryo, resulting in a hybrid organism having some cells with the new DNA and some with the unaltered [24].

2.2.2. Enabling Photostimulation in Neurons

In the biology literature, there are many applications in which cellular DNA has been altered to create genetically modified cells with new abilities. In this regard, we

[2] A marker gives the selected cells the ability to survive in a hostile environment such as a solution with growth inhibiting drug. In this case, the resistance allows the cells with the marker to continue growing, while others diminish. Similarly, other methods mentioned in this section also yield to cells that does not show the desired new properties. In that case, again, the selective markers are utilized to purify the outcome of the process.

elaborate on a series of experiments ultimately resulting in behavioral control of living fruit flies.

In [25,26], neurologists have succeeded in selectively stimulating neurons in terms of functionality. In order to achieve this, they have extracted Drosophila (Fruit fly) photoreceptor genes and introduced them to vertebrate neurons, making them responsive to visible light. Enabling remote stimulation in neurons has given the scientists to observe neural paths through selectively given probes to these neurons.

Later, in a succeeding study [27], neurologists have managed to use photo activated circuitry in Drosophila brain to induce involuntary behaviour. They managed to trigger characteristic escape behaviour of the fly by externally stimulating the reflex circuitry of the animal with visible light. In the study, even the decapitated flies have expressed the reflex behavior, which lead the authors to argue the use of similar methods to be studied as a remedy to functional impairments.

Lastly, in [28], Claridge *et al.* have developed a control mechanism for Dopaminergic neurons in Drosophila again by using photostimulation of the target cells. In this study the authors first located the responsible region for the aversive reinforcement in the fly and then artificially activated it, while subject to various odors to re-program (by means of forming an olfactory -smell related- memory) flies to display the desired behavior.[3]

The talents of genetic engineering empower scientists to create genetically engineered organisms which perform various tasks that almost feel unreal. In nanonetworking, we can utilize this phenomena to realize nano-communication between bioengineered cells. In this direction, enabling photostimulation is a promising candidate since it gives the researcher an active control mechanism over the communicating machines.

[3]Dopaminergic neurons: Neurons that contain or synthesize dopamine (A neurotransmitter often related conditional learning, especially in flies) or contain dopamine receptors.

2.3. Overview on Molecular Communication via Diffusion

Molecular communication via diffusion (MCvD) is extensively studied in the nano-communication literature for its wide array of applications and anticipated bio-compatibility. In this section, we provide an overview on MCvD, where biological and nanonetworking aspects of the paradigm are elaborated.

2.3.1. Basics of MCvD

MCvD systems are composed of modulation, emission (transmission), signal propagation, reception, and demodulation processes. The communication starts at the transmitter as it decides on the modulation type and the signal shape. The propagation environment is a viscous fluid (often water, blood, or similar bodily fluids) where Brownian Motion is the main means of molecular transfer. The propagation of molecules can be aided by flow currents (diffusion with drift) or turbulence, which often require non-linear modeling. The receiver is often modeled as a passive element, responsible for detecting the presence of the molecules and demodulating signal. In the literature, many receiver types are modeled as the nature of the modeling changes the behavior of the system through the change of the molecular arrival mechanics. The reception process is discussed in detail in Section 2.3.5.

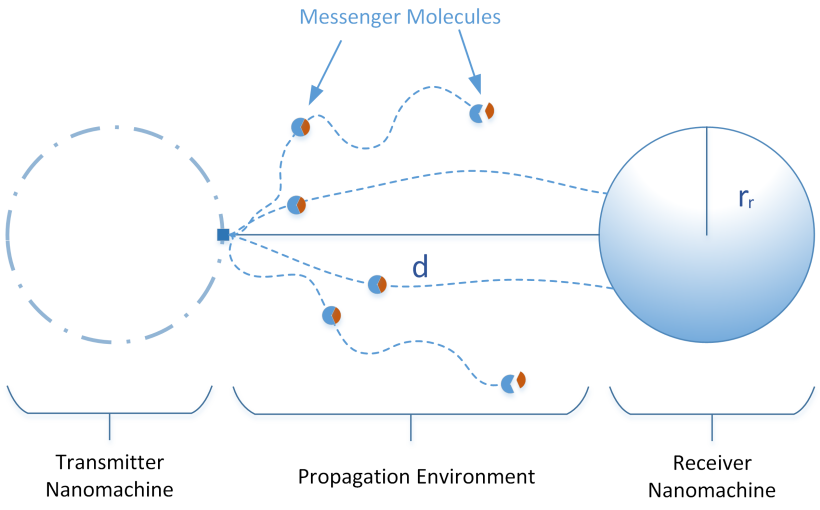

Figure 2.2. Molecular communication via diffusion schema.

Figure 2.2 sketches a basic MCvD system. In the figure, a spherical transmitter

nanomachine is depicted in dashed lines since in the literature transmitters are often taken as point sources. The propagation environment is the only link between the transmitter and receiver pair. The messenger molecules are often selected as simple compounds. However, they can be chosen as more complex compounds allowing molecular degradation. As seen in the figure, messenger molecules use random motion to travel through the propagation medium. Therefore, their arrival times show significant deviation. The late arriving molecules (stray molecules) from previous symbol durations often interfere with the current symbol durations and harm the demodulation process. Degradation eliminates stray molecules and results in a beneficial arrival pattern. The receiver nanomachine can be a point, rectangular prism, or a sphere. It can be absorbing (i.e. removing messenger molecules from the propagation environment upon impact) or concentration based (counting the amount of molecules inside the receiver volume).

2.3.2. Communication via Diffusion in Nature

Almost all of the communication in nature takes place in the form of molecular signaling. These signaling forms can be direct communication via diffusion, calcium signaling, secondary messenger signaling, pheromone signaling, etc. All of these forms, regardless of the purpose or name, utilize diffusion of messenger molecules -which may be Acetylcholine (ACh), Ca^{2+} ions, IP_3, 2,5-dimethylpyrazine (mouse [29])- for transmitting the desired message to the appropriate recipient.

2.3.3. Uses of Degradation in the Nature

The most typical use of molecular degradation in the nature is found in the synaptic cleft between the axons and the dendrites of the neurons in the brain. Some form of communication is needed to carry the action potential from the axon of the pre-synaptic neuron to the dendrite of the post-synaptic neuron. In this process, the pre-synaptic neuron, following the arrival of the action potential to the synapse, releases bursts of ACh molecules to the synaptic cleft. These ACh molecules diffuse across the synaptic junction and result in a new action potential in the post-synaptic neuron

after absorption.[4] The degradation in this case is introduced via the ACh hydrolyzing enzyme Acetylcholinesterase (AChE), which terminates the ACh action in the synaptic junctions. A single AChE molecule can terminate 6×10^5 ACh molecules per minute [30]. This is one of the fastest cases of degradation in the nature, and it is close to the theoretical limits of enzymatic hydrolysis [31].

By cleaning the communication channel from the messenger molecules, AChE enables the communication in the synaptic cleft to continue as the new wave of messenger molecules arrive in the channel. From a networking point of view, the presence of AChE reduces inter symbol interference (ISI) and greatly increases the overall bit rate of the system. Without the AChE presence, the channel overflows with ACh and the communication stops in the synaptic cleft. Therefore, the AChE and the degradation it causes is crucial to human life. Historically, anti-AChE agents (a.k.a nerve gases) have been used in wars to inhibit AChE activity as a deadly weapon [32].

2.3.4. Modulation Techniques in Molecular Communication

In the nanonetworking literature, information is demonstrated to be modulated on various aspects of the messenger molecules, such as molecule identity, molecule concentration, and signal frequency.

Most of the literature considers modulation based on the amplitude of the molecular concentration analogous to amplitude modulation (AM) in electromagnetic communication [33, 34]. Naming convention for this modulation is Concentration Shift Keying (CSK). In [35], a modulation technique based on molecule type is introduced as Molecular Shift Keying (MoSK), where different molecular arrangements of Hydrofluorocarbon molecules are used as messenger molecules for the sake of the example. In [36] and [37], a communication scheme in which the information is modulated on different discrete frequencies of the carrier wave is introduced. This modulation is called Molecular Frequency Shift Keying (MFSK).

[4] For a single burst $\sim 10^{-17}$ moles of ACh, roughly 6 million molecules, are released [30]

2.3.5. Modeling Diffusion for Different Receiver Types

In the molecular nano-communication literature, many authors use an approximate solution of the diffusion equation in order to model MCvD. Below we elaborate on these solutions and articulate their benefits and shortcomings.

Concentration Based Point Receiver. In many applications, the reception is modeled through a 3-D concentration based receiver. In this case the receiver considered is a point in space on which the concentration gradient is measured. The most significant advantage of this approximation is that it has the easiest derivation for the channel response. Following Fick's diffusion equation, the response for the input burst can be found as [38]

$$h(t) = p(d,t) = \frac{1}{(4\pi Dt)^{3/2}} \exp\left[-\frac{d^2}{4Dt}\right] \tag{2.1}$$

for the solution of

$$\partial_t\, p(d,t) = D\nabla^2 p(d,t) \tag{2.2}$$

with initial:

$$p(d, t \to 0) = \delta(d) \tag{2.3}$$

denoting the initial burst of molecules at $t \to 0$ and boundary condition

$$p(d \to \infty) = 0 \tag{2.4}$$

denoting the diminishing concentration at infinite distance. Notice that, even though this solution is in three dimensions, the concentration gradient is indifferent to the direction. The gradient symmetrically follows a Gaussian distribution with standard deviation $\sigma = \sqrt{2Dt}$ and mean $\mu = 0$, where D is the diffusion coefficient [39]. Although this method is easy to implement, it has major assumptions effecting the characteristic

of the received molecule distribution. First, it utilizes a dimensionless point receiver, which would not be the case in reality. Second, the final expression given in (2.1) has no dependence to the receiver size. Therefore, approximations regarding receivers of large size with small d fail at a significant rate. Third, it does not consider absorption of the messenger molecules, but the concentration around the receiver, which again is unrealistic. In the literature, many papers utilize this type of approximation (see [39–42]).

One Dimensional Infinite Absorbing Receiver. The second most used approximation is the 1-D infinite receiver case since it appropriately models a system in which the receiver radius r_r is significantly larger than d. The model considers an absorbing point as a receiver located at a distance d from a point transmitter, in a one-dimensional infinite environment. In this model, following the Wiener process presented in [43], one can reach the fraction of arriving molecules for an input burst at the transmitter as

$$h(t) = \frac{d}{\sqrt{4\pi D t^3}} \exp\left[-\frac{d^2}{4Dt}\right]. \tag{2.5}$$

This model is often utilized in the literature to model the amount of received molecules between two points of time. Notice that, different from (2.1), this equation considers the rate of absorption of the molecules by the receiver instead of measuring the momentary concentration, where in the latter case the amount of molecules in the system does not diminish.

The first downfall of this model is that it requires that the ratio of d/r_r approaches infinity, and therefore, it is not feasible for most of the receiver cases, since most of the considered receivers are in fact biological cells and have small radii. Second, as observed form (2.5), the fraction of received molecules approaches to 1 as $t \to \infty$, indicating every released molecules will eventually be absorbed. However, in the 3-D absorbing case, this value approaches to the ratio r_r/r_0, leaving some molecules in the system unreceived no matter how much time has passed. Here, r_0 is the distance of the transmitter to the center of the spherical receiver, satisfying $r_0 = r_r + d$. In the literature, many studies consider this approximation, where the number of absorbed

molecules are required in the model such as [34, 44, 45].

Concentration Based Volumetric Receiver. This type of approximation is derived based on the point concentration receiver, where a volumetric integral is used to find the number of molecules residing within the specified volume at a given time. The derivations are presented in [46] for the rectangular prism and the spherical volumes. The rectangular concentration can be found by integrating in each dimension as

$$h(t) = \frac{1}{8} \prod_{l \in x,y,z} \left(\text{erf}\left(\frac{l_f}{2\sqrt{t}} \right) - \text{erf}\left(\frac{l_i}{2\sqrt{t}} \right) \right), \tag{2.6}$$

where l_i and l_f are both ends of the sides of rectangular prism in each dimension (i.e. $x_f - x_i$ would be the length of the side of the prism in x-axis). The spherical concentration can be formulated utilizing the spherical coordinate system as

$$\begin{aligned} h(t) = &\frac{1}{2} \left[\text{erf}\left(\frac{-d}{2\sqrt{t}} \right) + \text{erf}\left(\frac{2r_r + d}{2\sqrt{t}} \right) \right] \\ &+ \frac{1}{r_0} \sqrt{\frac{t}{\pi}} \left[\exp\left(-\frac{(r_r + r_0)^2}{4t} \right) - \exp\left(-\frac{(r_0 - r_r)^2}{4t} \right) \right], \end{aligned} \tag{2.7}$$

where r_r is receiver radius, r_0 is the distance from the center of the sphere to the transmitter, and d is the shortest distance between transmitter, and the receiver, calculated as $d = r_0 - r_r$.

Although this receiver model is more accurate compared to the point concentration based counterpart, it is rarely used in the literature due to its complex formulation. Notice that this approximation, even though elaborate, still fails to consider molecule absorption.

Simulating Diffusion for Arbitrary Environments. This methodology is based on simulating individual molecule movements according to Brownian Motion, rather than trying to come up with a closed form solution. The simulation of the Brownian Motion can be derived from (2.1). As mentioned earlier, the displacement of a molecule follows a Gaussian distribution with $\mu = 0$ and $\sigma = \sqrt{2Dt}$. The simulation is built

upon the fact that when each molecule choses a random direction and moves following a Gaussian random variable $\Delta X \sim \mathcal{N}(0,\ 2D\Delta t)$, the overall movement of the concentration gradient follows the original Gaussian bell set by (2.1).[5] The variable Δt is called the step size and affects the size of the displacement of each molecule in each simulation step. Longer Δt yields faster simulations, providing a coarser grained representation of real molecule movement, whilst smaller time steps would allow a detailed modeling of the movement of the molecules.

The main benefit of using simulations is the ability to model the movement of molecules in any arbitrary environment, for which a closed form solution is hard to come up with, if not impossible. In the literature, many papers utilized simulation to model the molecule propagation in environments such as 3-D transmitter - 3-D absorbing receiver [35,47], two communicating pairs of 3-D transmitter and 3-D absorbing receiver [48], and a cylindrical tunnel between spherical transmitter - receiver pair [49].

Notice that in a simulation environment, in addition to arbitrary topology, we can model absorption or degradation by simply removing the molecules from the environment depending on their location (i.e. remove the ones crossing the receiver border) or their life-time (we can select an arbitrary distribution and utilize a random variable with that distribution to decide when to remove a messenger molecule). This approach gives extreme flexibility to the simulations. However, in order to effectively follow the restrictions imposed by the environment, the simulation step time should be selected very small (on the order of $\sim 10^{-6}$ s or smaller, which can increase the simulation durations, making it impractical. In order to remedy this issue, some of the research in the nanonetworking literature explores parallel and distributed simulators [50].

2.3.6. Molecular Degradation in Molecular Communication Literature

In the nanonetworking literature, molecular degradation has been considered conservatively. Although evidence in the nature can be found for cases where degradation

[5]Notice here that the sum of independent Gaussian random variables yields to a new Gaussian random variable following $\mathcal{N}(\sum_i \mu_i,\ \sum_i \sigma_i^2)$.

increases communication performance, the literature is divided in considering degradation as detrimental or beneficial.

In [44], Nakano *et al.* investigate the channel capacity of communication via diffusion, considering exponential degradation of the messenger molecules. Although they provide a solid formulation for the channel capacity, they only analyze a limited amount of scenarios with few performance metrics. In addition, their channel model is a 1-D approximation, failing to comprehensively model the effects of degradation in the system (see Section 2.3.5 for more information). In [34], a similar analysis is made for the case of a degradation pattern following a Weibull distribution, again using the 1-D absorber approximation.

In [51], Liu *et al.* provide a channel capacity analysis for the communication via diffusion with a receptor with ligand receptors. The use of ligand receptors entitles the consideration of binding and release rates of the messenger molecules to the ligands and the exponential degradation of these molecules in the propagation medium. In this study, again, the benefits of degradation is overlooked by only considering a very limited set of cases (exact number is 4). In this model, a concentration based receiver approximation is used in the channel response formulation.

In [46,52], Noel *et al.* make the analysis of the effects of enzymatic degradation of messenger molecules. This analysis is thorough in the sense that it models enzymatic reactions according to Michaelis-Menten mechanism, which is a highly accepted model of enzymatic degradation. Although this model covers the basis of benefits of degradation by stating the signal shaping aspect, it fails to deliver a complete mathematical derivation regarding the reason behind the improvements. In the study, the analysis is based on a single symbol duration, therefore fails to show the benefits of degradation in an ongoing communication scenario. Finally, this study utilizes an enhanced version of concentration based receiver, where the receiver is no longer a point in space but a finite volume (a sphere or a rectangular prism) in which the number of molecules are counted in bulk. In this model, there is not any absorption or manipulation of messenger molecules by the receiver.

3. HITTING RATE TO A SPHERICAL ABSORBER

3.1. Modeling the Molecular Channel without Degradation

The microscopic theory of diffusion can be developed from two simple assumptions. The first is that a substance moves down on its concentration gradient. A steeper gradient results in the movement of more particles. The derivative of the flux with respect to time results in Fick's Second Law in a 3-D environment,

$$\frac{\partial p(r,t|r_0)}{\partial t} = D\nabla^2 p(r,t|r_0), \tag{3.1}$$

where ∇^2, $p(r,t|r_0)$, and D are the Laplacian operator, the molecule distribution function at time t and distance r given the initial distance r_0, and the diffusion constant, respectively. The value of D depends on the temperature, viscosity of the fluid, and the Stokes' radius of the molecule [53].

For the calculation of the hitting rate to a spherical absorber, we consider the methodology presented in [54] and [55]. In the remainder of this section, we present the derivation of the formulas to ultimately find the fraction of molecules absorbed by the receiver as a function of time.

In addition to Fick's 3-D diffusion equation, we should define the initial and the boundary conditions obeying the problem at hand.

The initial condition is defined as

$$p(r,t\to 0|r_0) = \frac{1}{4\pi r_0^2}\delta(r-r_0), \tag{3.2}$$

and the first boundary condition is

$$\lim_{r\to\infty} p(r,t|r_0) = 0, \tag{3.3}$$

which denotes the assumption that the distribution of the molecules vanishes at distances far greater than r_0. The second boundary condition is

$$D\frac{\partial p(r,t|r_0)}{\partial r} = \alpha p(r,t|r_0) \text{ , for } r = r_r \tag{3.4}$$

for which as α, the rate of reaction, approaches infinity, we create a boundary where every collision leads to absorption. With the messenger molecules being absorbed on first contact with the cell surface, we consequently have a diminishing $p(r,t|r_0)$ as approaching to the surface of the absorber (i.e., $p(r_r,t|r_0) = 0$, which also holds as a boundary condition).

First, we observe that Fick's Second Law given in (3.1) becomes

$$\frac{\partial(r \cdot p(r,t|r_0))}{\partial t} = D\frac{\partial^2 r \cdot p(r,t|r_0)}{\partial r^2} \tag{3.5}$$

when we move to the spherical coordinates and drop the terms with θ and ϕ from the Laplacian operator, since $p(r,t|r_0)$ is spherically symmetric and depends solely on r.

As the next step, we partition $p(r,t|r_0)$ into two equations, $u(r,t|r_0)$ and $v(r,t|r_0)$, which individually obey the radial diffusion equation (3.5) and together obey the boundary conditions (3.3) and (3.4). Therefore, the function $u(r,t|r_0)$ must satisfy

$$\frac{\partial(r \cdot u(r,t|r_0))}{\partial t} = D\frac{\partial^2(r \cdot u(r,t|r_0))}{\partial r^2}, \tag{3.6}$$

$$r \cdot u(r,t \to 0|r_0) = \frac{1}{4\pi r_0}\delta(r - r_0). \tag{3.7}$$

Through Fourier transform, we obtain

$$r \cdot u(r,t|r_0) = \frac{1}{2\pi}\int_{-\infty}^{+\infty} \mathcal{U}(k,t|r_0)e^{ikr}dk. \tag{3.8}$$

By plugging (3.8) into (3.5), we get

$$\mathcal{U}(k,t|r_0) = K_u \cdot \exp[-Dtk^2] \tag{3.9}$$

where K_u is the time-independent coefficient. It is determined from the initial condition (3.7) as

$$K_u = \frac{1}{4\pi r_0} e^{-ikr_0}, \tag{3.10}$$

which results in the final Fourier expression

$$r \cdot u(r,t|r_0) = \frac{1}{8\pi^2 r_0} \int_{-\infty}^{+\infty} \exp[-Dtk^2] e^{ik(r-r_0)} dk \tag{3.11}$$

that yields the following expression after integration

$$r \cdot u(r,t|r_0) = \frac{1}{4\pi r_0} \frac{1}{\sqrt{4\pi Dt}} \exp\left[-\frac{(r-r_0)^2}{4Dt}\right]. \tag{3.12}$$

Secondly, we handle the remaining part, $v(r,t|r_0)$, which must satisfy

$$\frac{\partial(r \cdot v(r,t|r_0))}{\partial t} = D \frac{\partial^2 (r \cdot v(r,t|r_0))}{\partial r^2} \tag{3.13}$$

$$r \cdot v(r, t \to 0|r_0) = 0. \tag{3.14}$$

Through Laplace transform this time, we have

$$\frac{s}{D}(r \cdot \mathcal{V}(r,s|r_0)) = \frac{\partial^2 (r \cdot \mathcal{V}(r,s|r_0)}{\partial r^2}, \tag{3.15}$$

where $\mathcal{V}(r,s|r_0)$ is the Laplace transform of $v(r,t|r_0)$. Applying the boundary condition (3.3), we obtain

$$r \cdot \mathcal{V}(r,s|r_0) = K_v \exp\left[-\sqrt{\frac{s}{D}} r\right], \tag{3.16}$$

where K_v is a constant that should satisfy the second boundary condition (3.4). At this point, we consider the transform of the complete solution $p(r,t|r_0)$ rather than the inverse Laplace transform of $v(r,t|r_0)$, since from the boundary condition it is easier to determine the arbitrary constant K_v. Here, we finally plug in the Laplace transform of $u(r,t|r_0)$ and obtain

$$\begin{aligned} r\cdot\mathcal{P}(r,s|r_0) &= r\cdot\mathcal{U}(r,s|r_0)+r\cdot\mathcal{V}(r,s|r_0), \\ &= \frac{1}{4\pi r_0}\frac{1}{\sqrt{4Ds}}\exp\left[-\sqrt{\frac{s}{D}}|r-r_0|\right] \\ &\quad + K_v\exp\left[-\sqrt{\frac{s}{D}}r\right]. \end{aligned} \tag{3.17}$$

Also with the Laplace transform of the boundary condition (3.4), we get

$$\left.\frac{\partial(r\cdot\mathcal{P}(r,s|r_0))}{\partial r}\right|_{r=r_r} = \frac{\alpha r_r+D}{Dr_r}r_r\cdot\mathcal{P}(r,s|r_0). \tag{3.18}$$

From (3.17) and (3.18), we determine

$$\begin{aligned} K_v = &\frac{\sqrt{s/D}-(\alpha r_r+D)/(Dr_r)}{\sqrt{s/D}+(\alpha r_r+D)/(Dr_r)}\frac{1}{4\pi r_0}\frac{1}{\sqrt{4Ds}} \\ &\times\exp\left[-\sqrt{s/D}(r_0-2r_r)\right] \end{aligned} \tag{3.19}$$

which produces the ultimate result for $\mathcal{P}(r,s|r_0)$. The inverse Laplace transform of $\mathcal{P}(r,s|r_0)$ yields to

$$\begin{aligned} p(r,t|r_0) = &\frac{1}{4\pi r r_0}\frac{1}{\sqrt{4\pi Dt}}\left(\exp\left[-\frac{(r-r_0)^2}{4Dt}\right]+\exp\left[-\frac{(r+r_0-2r_r)^2}{4Dt}\right]\right) \\ &-\frac{1}{4\pi r r_0}\frac{\alpha r_r+D}{Dr_r}\exp\left[\left(\frac{\alpha r_r+D}{Dr_r}\right)^2 Dt+\frac{\alpha r_r+D}{Dr_r}(r+r_0-2r_r)\right] \\ &\times\operatorname{erfc}\left[\frac{\alpha r_r+D}{Dr_r}\sqrt{Dt}+\frac{r+r_0-2r_r}{\sqrt{4Dt}}\right]. \end{aligned} \tag{3.20}$$

Now, for the case of the absorbing boundary, we consider the case when $\alpha\to\infty$

and the solution (3.20) becomes

$$p(r,t|r_0) = \frac{1}{4\pi r r_0}\frac{1}{\sqrt{4\pi D t}} \times \left(\exp\left[-\frac{(r-r_0)^2}{4Dt}\right] - \exp\left[-\frac{(r+r_0-2r_r)^2}{4Dt}\right]\right). \tag{3.21}$$

Following the molecule distribution $p(r,t|r_0)$, we find the hitting rate of the molecules $h(\Omega_r,t|r_0)$ to the receiver Ω_r, which is given by

$$\begin{aligned} h(\Omega_r,t|r_0) &= 4\pi r_r^2\, p(r_r,t|r_0) \\ &= \frac{r_r}{r_0}\frac{1}{\sqrt{4\pi D t}}\frac{r_0-r_r}{t}\exp\left[-\frac{(r_0-r_r)^2}{4Dt}\right]. \end{aligned} \tag{3.22}$$

Furthermore, by integrating $h(\Omega_r,t|r_0)$ we obtain the fraction of molecules absorbed by the receiver until time t, $w(\Omega_r,t|r_0)$

$$\begin{aligned} w(\Omega_r,t|r_0) &= \int_0^t h(\Omega_r,t'|r_0)dt' \\ &= \frac{r_r}{r_0}\mathrm{erfc}\left[\frac{r_0-r_r}{\sqrt{4Dt}}\right]. \end{aligned} \tag{3.23}$$

Hence, the expected fraction of molecules hitting to the receiver in an interval $[t_1,t_2]$ can be evaluated by

$$w_c(\Omega_r,t_1,t_2|r_0) = w(\Omega_r,t_2|r_0) - w(\Omega_r,t_1|r_0), \tag{3.24}$$

which gives the expected number of molecules that arrive between t_1 and t_2 when multiplied with the number of initially released molecules, $N_{\mathrm{Tx}}^{r_0}$.

3.2. Incorporating Molecular Degradation

In the biology literature, degradation of a molecule has been extensively studied as a part of an enzymatic process. Although there are many advanced models for enzymatic decay [56, 57], we utilize exponential decay function in order to constitute a generic model about degradation, not confined by enzymatic hydrolysis. In our model, if a messenger molecule degrades before it reaches the receiver, it does not cause a reaction and is not considered as one of the received molecules. Therefore, degradation inevitably reduces the amount of molecules received in a given time frame. Since every molecule undergoes a form of degradation, ignoring degradation results in a false interpretation of the communication process.

To incorporate molecular degradation into MCvD, we start with the generic exponential decay function

$$C(t) = C_0 e^{-t\lambda}, \tag{3.25}$$

where C_0 is the initial concentration, $C(t)$ is the concentration at time t, and λ is the rate of degradation. While C_0 is given as the number of molecules, λ is calculated as follows from the corresponding half-life ($\Lambda_{1/2}$) of the messenger molecules:

$$\lambda = \frac{\ln(2)}{\Lambda_{1/2}}. \tag{3.26}$$

To find the amount of molecules collide with the receiver before degradation, we employ basic probability of succession in events. If A and B are independent events, the probability that event A occurs before event B can be found by

$$\int_0^\infty f_A(t) \cdot P_B(T > t) dt. \tag{3.27}$$

In our case, the events A and B are the arrival of the messenger molecule at the receiver and its degradation, respectively. We are interested in the probability that a molecule arrives at the receiver before getting degraded. Therefore, we are dealing

with *not getting degraded (survival) before the arrival time* and $P_B(T > t)$ corresponds to the event of degradation time being greater than arrival time t. These two events are independent since neither the survival event affects the reception probability nor the reception itself affects exponential degradation.[6] The probability of not getting degraded can be found by the complementary cdf (ccdf) of the exponential distribution as:

$$\bar{F}(t) = 1 - F(t) = 1 - P(T < t) = 1 - (1 - e^{-\lambda t}) = e^{-\lambda t} \tag{3.28}$$

Thus, the new channel response function can be easily expressed as:

$$h(\Omega_r, \lambda, t|r_0) = \frac{r_r}{r_0} \frac{1}{\sqrt{4\pi D t}} \frac{r_0 - r_r}{t} \exp\left[-\frac{(r_0 - r_r)^2}{4Dt} - \lambda t \right]. \tag{3.29}$$

Following (3.29), the combined probability of getting absorbed before getting degraded can be found as

$$\begin{aligned} w(\Omega_r, \lambda|r_0) &= \int_0^\infty h(\Omega_r, \lambda, t|r_0)\, dt \\ &= \int_0^\infty h(\Omega_r, t|r_0)\, e^{-\lambda t}\, dt. \end{aligned} \tag{3.30}$$

One can observe (3.30) is conveniently the Laplace transform of $h(\Omega_r, t|r_0)$, and yields itself to

$$w(\Omega_r, \lambda|r_0) = \frac{r_r}{r_0} \exp\left[-\sqrt{\frac{\lambda}{D}}(r_0 - r_r) \right]. \tag{3.31}$$

To further detail our problem, we investigate the probability of colliding with the receiver before exponential degradation and before an arbitrary time t, which is the degradation enabled counterpart of (3.23) and gives the fraction of initial molecules

[6] Notice that, this is not the case, i.e. the events are dependent, if the events are defined as getting-degraded and reception. In this case, probability of reception is preceded by the degradation since a degraded molecule cannot be received.

that are absorbed by the receiver until time t for the release at $t_0 = 0$.

$$\begin{aligned} w(\Omega_r, \lambda, t|r_0) &= \int_0^t h(\Omega_r, \lambda, t'|r_0)\, dt' \\ &= w(\Omega_r, \lambda|r_0) - \frac{r_r}{2r_0} \cdot e^{-\sqrt{\frac{\lambda}{D}}(r_0 - r_r)} \\ &\times \left\{ \operatorname{erf}\left(\frac{r_0 - r_r}{\sqrt{4Dt}} - \sqrt{\lambda t} \right) + e^{2\sqrt{\frac{\lambda}{D}}(r_0 - r_r)} \right. \\ &\times \left. \left[\operatorname{erf}\left(\frac{r_0 - r_r}{\sqrt{4Dt}} + \sqrt{\lambda t} \right) - 1 \right] + 1 \right\}. \end{aligned} \tag{3.32}$$

For validation, one can first check that the t dependent part of (3.32) expectedly approaches to 0 as $t \to \infty$ and satisfies $w(\Omega_r, \lambda, t \to \infty|r_0) = w(\Omega_r, \lambda|r_0)$. Second, it converges to $w(\Omega_r, t|r_0)$ as $\lambda \to 0$ or $\Lambda_{1/2} \to \infty$; thus, meeting the case with no degradation.

Lastly, in order to model the expected number of arrivals during a time frame (later to be named the symbol duration), we define the discrete channel response w_c from an arbitrary t_1 to t_2 as:

$$w_c(\Omega_r, \lambda, t_1, t_2|r_0) = w(\Omega_r, \lambda, t_2|r_0) - w(\Omega_r, \lambda, t_1|r_0), \tag{3.33}$$

which is formally the fraction of molecules that arrive in the time interval of $[t_1, t_2]$ for a symbol that was sent at time t_0, where $t_0 \leq t_1 < t_2$.

Figure 3.1 plots the number of arriving molecules with respect to time, and their behavior under two different degradation scenarios with $\Lambda_{1/2} = 0.016\ s$ and $\Lambda_{1/2} = 0.128\ s$. The figure is plotted using w_c evaluated at discrete intervals of 10^{-3} seconds (i.e. $w_c(\Omega_r, \lambda, t, t + 10^{-3}|r_0)$ is evaluated for every discrete t from 0 to 0.2 with 0.001 increments) for a initial release of $N = 100\,000$ molecules. The simulations conducted for the same topology using a step size of $\Delta t = 10^{-6}$ seconds and for every 1000 step the received molecules are summed and reported. The simulation results expectedly display small deviations from the mean value, that is represented by the analytical formula.

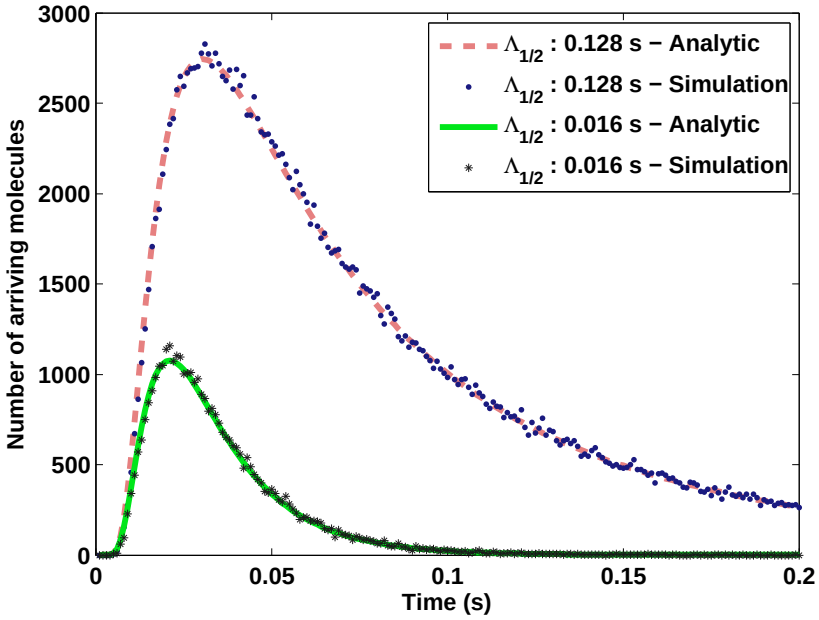

Figure 3.1. Hit time histogram of the messenger molecules for an initial release of $N = 100\,000$ molecules. Analytic solution indicates the expected value of the arrivals.

4. CHARACTERISTICS OF THE MOLECULAR DIFFUSION CHANNEL

In this chapter, we first elaborate on the observations derived from the changes in the shape of the molecular signal with and without degradation. Second, we introduce the general continuous communication model we use, when we evaluate the performance of the various systems in Chapter 5.

4.1. Shape of the Molecular Signal

In diffusion based communication, due to the uncontrollable nature of the Brownian Motion of messenger molecules, signal shaping is hard to achieve. However, with the introduction of molecular degradation, we are shaping the MCvD signal into a more desirable form with less stray molecules and shorter peak time. In this section, we elaborate on the effects of degradation onto the shape of the signal.

4.1.1. Pulse Peak Time

MCvD signal has one peak as shown in Figure 3.1. Hence, we can find the mean pulse peak time, t_{peak}, by finding the vanishing point for the derivative of $h(\Omega_r, \lambda, t|r_0)$ with respect to time:

$$\frac{\partial h(\Omega_r, \lambda, t|r_0)}{\partial t} = \partial_t \left(\frac{r_r}{r_0} \frac{d}{\sqrt{4\pi D t^3}} \, e^{-d^2/4Dt} e^{-\lambda t} \right) = 0. \tag{4.1}$$

While calculating $\partial_t h(\Omega_r, \lambda, t|r_0)$, we arrive at one crucial intermediate step:

$$\frac{r_r}{r_0} \frac{d}{\sqrt{4\pi D}} \left\{ t^{-3/2} \exp\left[-\frac{d^2}{4Dt} - \lambda t \right] \left(-\frac{3}{2t} + \frac{d^2}{4Dt^2} - \lambda \right) \right\} = 0 \tag{4.2}$$

Solving for t requires:

$$-\frac{3}{2t}+\frac{d^2}{4Dt^2}-\lambda=0. \tag{4.3}$$

Revising (4.3) gives us the quadratic equation:

$$4D\lambda t^2+6Dt-d^2=0 \tag{4.4}$$

At this point, one can evaluate (4.4) in two ways. First, if we consider the regular diffusion process where $\lambda=0$, we observe the coefficient on t^2 vanishes, leading to

$$\mathbb{E}[t_{\text{peak}}]=\frac{d^2}{6D}. \tag{4.5}$$

Second, if molecular degradation is considered, and $\lambda\neq 0$, the solution for t_{peak} becomes:

$$\mathbb{E}[t_{\text{peak}}|\lambda]=\frac{\sqrt{36D^2+16Dd^2\lambda}-6D}{8D\lambda}. \tag{4.6}$$

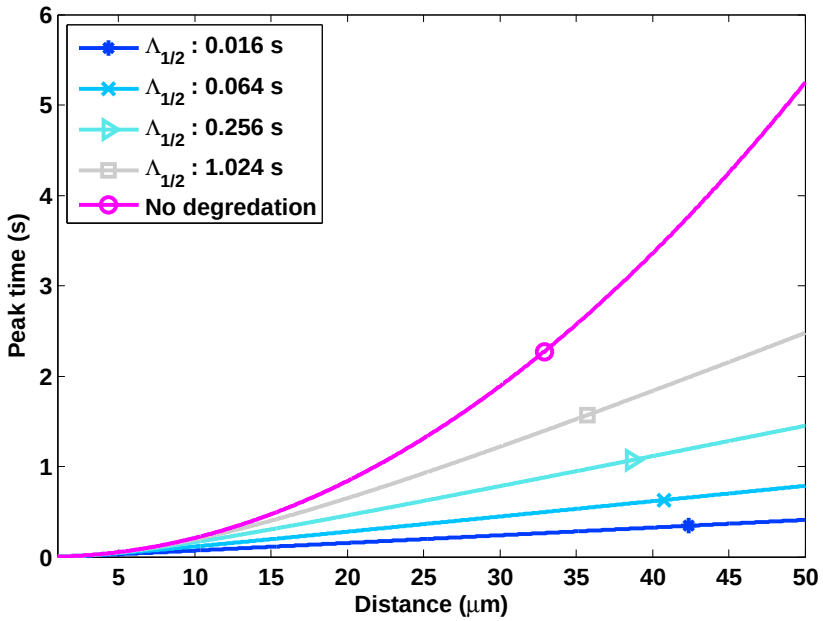

Figure 4.1. Distance versus peak time of the signal.

In electromagnetic (EM) communications, t_{peak} is proportional to the propaga-

tion time, which is the distance divided by the wave propagation speed, hence it is proportional to d. In the molecular communication system without degradation, due to the diffusion dynamics, t_{peak} is proportional to d^2. However, with the introduction of the degradation (even if the degradation process is very slow) this proportion again reduces to d. Thus, one can conclude that ignoring molecular degradation, as most of the previous work in the literature, results in a quite different signal shape. Furthermore, with the introduction of degradation, we can passively shape the molecular signal and reduce the restricting effect of diffusion dynamics on the signal travel time.

In Figure 4.1, distance versus $\mathbb{E}[t_{\text{peak}}]$ is depicted for different degradation scenarios. In the figure, we can observe that without degradation, the change in the peak time with respect to the distance is quadratic whereas it is linear when messenger molecules undergo degradation.

4.1.2. Pulse Amplitude

The pulse amplitude is the maximum amount of arriving molecules in a fixed size time frame. n_{peak} can be considered as the amount of molecules left after the channel attenuation, which is highly dependent on the communication distance.

Since the molecule arrivals to the absorbing receiver is a counting process, we cannot deal with the number of arriving molecules at a single point in time.[7] Instead, we must define an interval for which the number of arrivals are highest among all other intervals of the same length. To accomplish this, we start with t_{peak} where the highest amplitude is most likely to be observed. Then, we take the channel response between

[7]The diffusion process should be evaluated differently for the non-absorbing (concentration based) receiver since in the concentration based receiver we can conclusively decide the amount of molecules that are in the receiver zone at any instance of time, which nullifies the requirement for the small time window. However, although it may seem easier to model, the non-absorbing case is not a satisfactory model since it diverges receiver dynamics from reality. For example, n_{peak} would not depend on diffusion coefficient,D, contrary to the absorbing receiver case. However, the diffusion coefficient has a significant impact that can be determined experimentally [54, 58]. In addition, almost all of the MCvD receivers found in nature are absorbing or behave as one.

a time frame of $-\xi/2$ and $+\xi/2$ from t_{peak}. If we formulate n_{peak} we find

$$\mathbb{E}[n_{\text{peak}}] = N_{\text{Tx}}^{r_0}\, \xi\, h(\Omega_r, \lambda, t_{\text{peak}}|r_0) \tag{4.7}$$

where $N_{\text{Tx}}^{r_0}$ is the number of molecules that are initially released. The value of n_{peak} in this case depends on the receiver node radius r_r, distance d, degradation constant λ, and diffusion coefficient D.

At this point we again need to separate cases with and without degradation. For the latter, the calculation of $\mathbb{E}[n_{\text{peak}}]$ is neater, the end result yielding to:

$$\mathbb{E}[n_{\text{peak}}] = N_{\text{Tx}}^{r_0}\, \xi\, \frac{r_r}{d + r_r} \frac{D}{d^2} \frac{e^{-3/2}}{\sqrt{\pi/54}}. \tag{4.8}$$

For a fixed r_r, we have $n_{\text{peak}} \sim 1/d^3$. This behavior reveals the difference compared to EM communications. If we ignore fading, the amplitude of EM pulse propagating in free space decreases proportional to the square of the transmission distance. The amplitude of a pulse in the MCvD channel, however, decreases proportional to the cube of the distance.

Secondly, we calculate the peak amplitude of the degradation scenario using (4.6), which yields to the rather complicated equation

$$\begin{aligned}\mathbb{E}[n_{\text{peak}}|\lambda] = N_{\text{Tx}}^{r_0}\, \xi\, \frac{r_r}{r_r + d} & \frac{d}{\sqrt{4\pi D\, (\frac{\sqrt{36D^2 + 16Dd^2\lambda} - 6D}{8D\lambda})^3}} \\ & \times \exp\left[-\frac{2\lambda d^2}{\sqrt{36D^2 + 16Dd^2\lambda} - 6D} - \frac{\sqrt{36D^2 + 16Dd^2\lambda} - 6D}{8D} \right]\end{aligned} \tag{4.9}$$

where this time for a given r_r we have $n_{\text{peak}} \sim \frac{1}{d^{3/2}\, e^d}$ while λ being the factor on d.

In Table 4.1 we summarize the comparison for propagation time and path loss. In terms of data rate, MCvD without degradation has a clear disadvantage as, first,

Table 4.1. Diffusion channel characteristics comparison matrix.

Metric	Physical Relation	Electromagnetic	MCvD	MCvD with degradation
t_{peak}	Propagation Time	d	d^2	d
n_{peak}	Path Loss	$1/d^2$	$1/d^3$	$\frac{1}{d^{3/2}\, e^d}$

the propagation time of the information is proportional to the square of the distance and second, the path loss is one order of magnitude larger. Introducing degradation to the MCvD system seems to mitigate the issue with the propagation time, at the cost of exponential decrease in the peak amplitude with respect to distance. This indicates long distance communications would not favor high degradation rates, while short distance communications benefit from it.

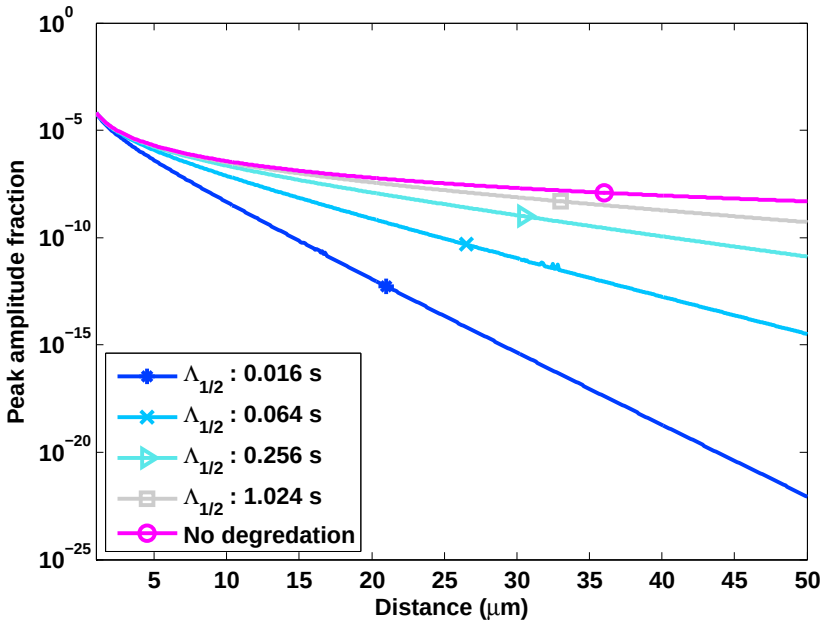

Figure 4.2. Distance versus peak amplitude of the signal for $\xi = 10^{-6}$ s.

Figure 4.2 depicts distance versus peak pulse amplitude fraction of $N_{\text{Tx}}^{r_0}$ for various degradation scenarios. We observe the rate of decrease in fast degradation cases is much higher than those with slow or no degradation. At this point we might argue the choice of degradation rate. Clearly, the $\Lambda_{1/2} = 0.016$ s case would not work well for a distance of 50 micrometers, since detection at the receiver site would not be easy. However, if we choose a degradation level of $\Lambda_{1/2} = 1.024$ s, we gain twice in propagation speed, while losing 10 times more molecules compared to the no degradation case. Although this seems like a non-favorable scenario, the energy consumption of producing 10 times more

molecules would be acceptable for an animal cell since the energy cost of messenger molecule creation is minuscule [47].

To conclude, introducing messenger molecule degradation to a MCvD system, allows the designer of the nano-network to shape the molecular signal in the propagation environment. This signal shaping especially benefits the channel in mitigating inter symbol interference (ISI) and providing a more clear signal for the receiver. We will elaborate on this in more detail in Chapter 5 after we conclusively model the channel in the remainder of this chapter.

4.2. Modeling the Arrival of a Single Burst of Molecules

The formulations derived in Sections 3.1 and 3.2 represent the expected fraction of molecules that arrive at the receiver until time t. When we incorporate the stochastic nature of the diffusion process, we conclude that the number of arrivals is a Binomial random variable where the success probability is w and number of trials is $N_{\text{Tx}}^{r_0}$.[8]

$$N_{\text{Rx}}^{\Omega_r}(0,t) \sim \begin{cases} \mathcal{B}(N_{\text{Tx}}^{r_0}, w(\Omega_r, \lambda, t|r_0)) & \text{with degradation} \\ \mathcal{B}(N_{\text{Tx}}^{r_0}, w(\Omega_r, t|r_0)) & \text{without degradation} \end{cases} \tag{4.10}$$

where $N_{\text{Rx}}^{\Omega_r}(0,t)$ is the number of received molecules between $[0,\ t)$ and $\mathcal{B}(n,p)$ is the Binomial random variable with n trials and success probability p.

Following from Binomial modeling, we observe the expected number of molecules that arrive until time t becomes

$$\mathbb{E}[N_{\text{Rx}}^{\Omega_r}(0,t)] = \begin{cases} N_{\text{Tx}}^{r_0} \cdot w(\Omega_r, \lambda, t|r_0) & \text{with degradation} \\ N_{\text{Tx}}^{r_0} \cdot w(\Omega_r, t|r_0) & \text{without degradation} \end{cases} \tag{4.11}$$

where $\mathbb{E}[.]$ and $N_{\text{Tx}}^{r_0}$ are the expectation operator and the number of released molecules,

[8] Here, w stands for the fraction of arrivals to the receiver. It should be interpreted as $w(\Omega_r, t|r_0)$ if there is not any degradation in the channel, and $w(\Omega_r, \lambda, t|r_0)$, otherwise. From here on, we use w in this short-hand notation where the existence of degradation is irrelevant.

respectively.

At this point, following the property of independent trials of the Binomial process, we observe that w can also be interpreted as the probability of a molecule being absorbed before time t. Furthermore, when we conduct $N_{\text{Tx}}^{r_0}$ trials with a single molecule in a simulation environment, we see that at time t on the average, $N_{\text{Tx}}^{r_0} \cdot w$ of the initial $N_{\text{Tx}}^{r_0}$ end up being absorbed. Therefore, for simulating or modeling diffusion, one may choose to repeat many trials for a small number of molecules or a small number of trials with many molecules to arrive at the same conclusion, ultimately using number of molecules and trials interchangeably.

4.3. Modeling Continuous Communication

4.3.1. Modulation and Demodulation

In order to understand the effect of molecular degradation, we design a communication scenario under basic operational constraints. First, we assume the time is divided into equal length time slots at which one bit is sent through the molecular channel. In this scenario we assume the transmitter and the receiver are fully synchronized, as explained in [39].

In the communication scenario, we use Concentration Shift Keying (CSK) since it is the most basic and widely applied technique. In this technique, we modulate the information on the amount of messenger molecules that are received in a symbol duration (t_s). This modulation type is analogous to Amplitude Modulation (AM) in electromagnetic communication and require a thresholding based demodulator.

The most straightforward use of CSK is the Binary CSK modulation scheme where two levels of concentration are used to modulate 1-bit information. In our scenario, we erupt a vesicle with N_0 molecules to represent a bit-0 and N_1 molecules to represent a bit-1. In order to increase the gap between N_0 and N_1 we choose $N_0 = 0$ and $N_1 = N_{\text{Tx}}^{r_0}$, where $N_{\text{Tx}}^{r_0}$ is the maximum number of molecules that can safely be

released from a cell in a single signal burst.

On the demodulation side, we assume that the receiver counts the number of molecules received for each symbol duration and compares that with the predetermined threshold τ. As previously described in Section 4.2, the number of molecules arriving at the receiver in the ith symbol duration is a binomial random variable, denoted by Y_i. The receiver demodulates i^{th} bit value as "0" if $Y_i \leq \tau$ and as "1" otherwise.

$$\mathcal{D}(Y_i) = \begin{cases} 0, & Y_i \leq \tau \\ 1, & \text{otherwise} \end{cases} \tag{4.12}$$

where $\mathcal{D}(.)$ represents the demodulation function for the received molecules.

4.3.2. Detection Probabilities

Number of received molecules in one symbol duration is originally binomially distributed as explained in Section 4.2. The parameters of the binomial distribution come from (3.32) and the number of released molecules. If bit-1 is sent in a symbol duration, we can formulate the correct detection probability of bit-1 as

$$Pc_1(\tau, \lambda, t_i | s_i = 1) = 1 - Pr(Y_i \leq \tau) \tag{4.13}$$

where, Y_i is the number of received molecules in the ith symbol duration. Therefore, if we consider only the molecules released in the ith symbol duration and discard the effect of previous symbol emissions, the probability of correct detection of a bit-1 becomes:

$$\begin{aligned} Pc_1(\tau, \lambda, t_i | s_i = 1) &= 1 - Pr(Y_i \leq \tau) \\ &= 1 - \sum_{k=0}^{\tau} \binom{N_1}{k} w^k \ (1-w)^{N-k} \end{aligned} \tag{4.14}$$

where, N_1 is the number of molecules sent to represent a bit-1.

In reality, Y_i is affected by the previous emissions, hence we have to incorporate all the molecules in the environment that are sent in a previous symbol duration. The new formula, for the ith symbol becomes:

$$\begin{aligned} Pc_1(\tau, \lambda, t_i | s_i = 1) &= 1 - Pr(Y_i \leq \tau) \\ &= 1 - Pr(Y_i^1 + ... + Y_i^m \leq \tau) \end{aligned} \tag{4.15}$$

where, Y_i^m values are the number of received molecules in ith symbol duration due to emission at the mth symbol duration. Y_i^m's are also binomially distributed random variables. This formula for correct detection of the ith bit, requires a recursive algorithm to work and does not have a closed form formula [59]. For this reason we employ a well known approximation of Binomial distribution to Poisson distribution as

$$\mathcal{B}(n, p) \sim \mathcal{P}(np) \tag{4.16}$$

This approximation is known to be successful in the case of large n and small p which are in our problem the number of molecules sent in each symbol duration and the fraction of arrivals. With this approximation we can derive a close form solution for the correct detection probability of bit-1 in the ith symbol duration as

$$Pc_1(\tau, \lambda, t_i | s_i = 1) = 1 - \left(e^{-N_1 \, w_s} \sum_{k=0}^{\tau} \frac{[N_1 w_s]^k}{k!} \right) \tag{4.17}$$

where, N_1 is the number of molecules sent to represent bit-1 and $w_s(\Omega_r, \lambda, t_k | r_0)$ is the sum of all channel responses that represent bit-1 until the ith symbol and the current symbol itself. Since we modulate bit-0 with emission of zero molecules, we just sum the emissions due to bit-1. $w_s(\Omega_r, \lambda, t_k | r_0)$ can be calculated as:

$$w_s(\Omega_r, \lambda, t_i | r_0) = \sum_{j=0}^{i-1} w_c(\Omega_r, \lambda, t_{i-j-1}, t_{i-j} | r_0) \, s_{i-j} \tag{4.18}$$

where, t_i is the point in time where ith symbol duration ends, i.e. $t_i = i \, t_s$ where t_s is the symbol duration, and s_m is the bit value of the mth bit.

Given this calculation for Pc_1, one easily derives Pc_0 for the ith symbol as

$$Pc_0(\tau, \lambda, t_i | s_i = 0) = e^{-N_1 w_s} \sum_{k=0}^{\tau} \frac{[N_1\, w_s]^k}{k!}. \tag{4.19}$$

Lastly, in order to derive the overall error probabilities for the channel, we calculate the average of all errors presented thus far and conclude

$$Pc_0(\tau, \lambda) = \lim_{i \to \infty} \sum_{z=0}^{i} \frac{Pc_0(\tau, \lambda, t_z | s_z = 0)}{i\, P(s_z = 0)} \tag{4.20}$$

and

$$Pc_1(\tau, \lambda) = \lim_{i \to \infty} \sum_{z=0}^{i} \frac{Pc_1(\tau, \lambda, t_z | s_z = 1)}{i\, P(s_z = 1)}. \tag{4.21}$$

The diffusion channel is significantly affected by the long tail of the arrival distribution of the molecules. The number of arriving molecules in each symbol duration is determined by the collective sum of arrivals from all previously sent symbols in the channel and their order of appearance.[9] Consequently, the detection of an arbitrary symbol in a communication scenario is heavily influenced by the preceding symbols. This is why (4.20) and (4.21) have no close form and can only be numerically evaluated. Luckily, in such a channel, (4.20) and (4.21) experience a fast convergence to an accurate value.

In Figure 4.3, we present the probability of correct detection for various threshold values. The figure indicates clear agreement between the simulation results and the Poisson model, whilst the Gaussian model, abundantly found in literature [40, 42], displays a higher margin of error. The reason behind is that the degradation, in general, lowers the expected number of arriving molecules and the Gaussian model is error prone in small numbers. Concerning the molecular channel, we observe that the

[9] To exemplify, the amount of stray molecules left for current symbol duration will be more if the preceding sequence of bits are '1111' rather than '0000'.

optimal threshold values are between $[10, 20]$ where Pe drops down to 0. As we go left, we observe a decline as a result of increased Pe_0 since smaller threshold values tend to err in favor of bit-1. Similarly, the right tail of the curve is bound by Pe_1 where larger thresholds result in increased number of false alarms.

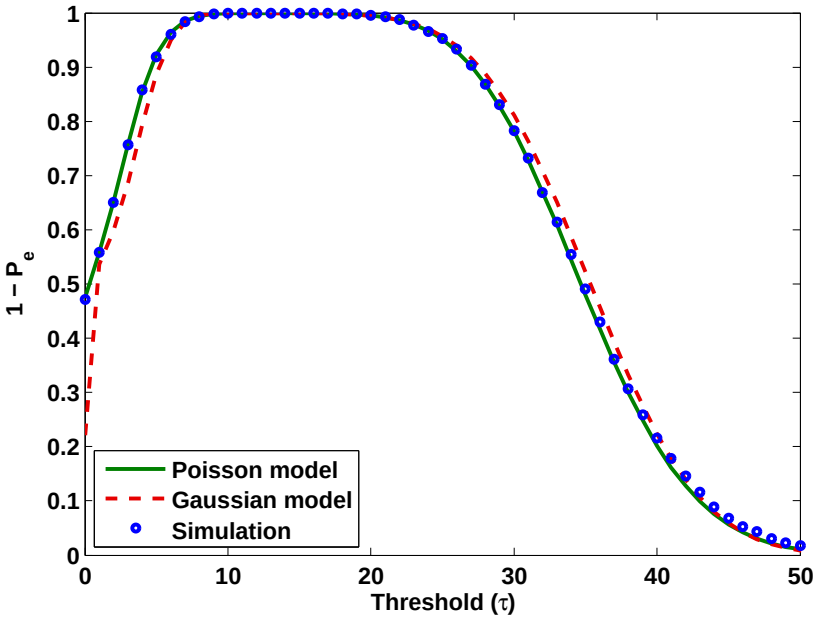

Figure 4.3. $1 - Pe$ for various thresholds (τ) with system parameters: $t_s = 0.6\ s$, $d = 4\ \mu m$, $N_1 = 1000$ and $\Lambda_{1/2} = 0.016\ s$. We observe clear similarity between simulation results and Poisson model presented through (4.13) to (4.21).

5. PERFORMANCE ANALYSIS OF DEGRADATION

5.1. Ratio of Unreceived Molecules

ISI is one of the biggest causes of communication impairment in CvD systems. Stray molecules from previous symbol durations pile up and impair the correct reception ability of the receiver. Utilizing degradation helps removing these molecules, creating a better system performance. In order to formulate the amount of stray molecules remaining in the system we create a new metric, $r(\Omega_r, \lambda, t|r_0)$ denoting the ratio of molecules that remain unreceived for one burst of molecules. $r(\Omega_r, \lambda, t|r_0)$ is formulated as follows in terms of the channel response functions:

$$r(\Omega_r, \lambda, t|r_0) = 1 - \frac{w(\Omega_r, \lambda, t|r_0)}{w(\Omega_r, \lambda, t \to \infty|r_0)}. \tag{5.1}$$

Using (3.31), (3.32), and (5.1) we come up with the slightly simpler expression

$$\begin{aligned} r(\Omega_r, \lambda, t|r_0) &= \frac{1}{2}\left\{\text{erf}\left(\frac{r_0 - r_r}{\sqrt{4Dt}} - \sqrt{\lambda t}\right) + e^{2\sqrt{\frac{\lambda}{D}}(r_0 - r_r)}\right. \\ &\times \left.\left[\text{erf}\left(\frac{r_0 - r_r}{\sqrt{4Dt}} + \sqrt{\lambda t}\right) - 1\right] + 1\right\} \end{aligned} \tag{5.2}$$

for the fraction of unreceived molecules. Notice that (5.2) is independent of r_0 and r_r individually, but dependent on $d = r_0 - r_r$, the distance between the transmitter and the receiver. Therefore, we conclude that observations derived from $r(\Omega_r, \lambda, t|r_0)$ metric are valid regardless of the receiver size as long as the distance is known.

Figure 5.1, depicts $r(\Omega_r, \lambda, t|r_0)$ for various half-life values where faster degradation clearly reduces the amount of stray molecules for a given molecular communication scenario. As observed from the figure, utilization of molecular degradation with $\Lambda_{1/2} = 0.016\ s$ clears almost all of the stray molecules in the system at $t = 0.2$ seconds. However, in the no degradation case more than half of the initially released molecules are still in the channel, unreceived, resulting in a channel with significant ISI especially

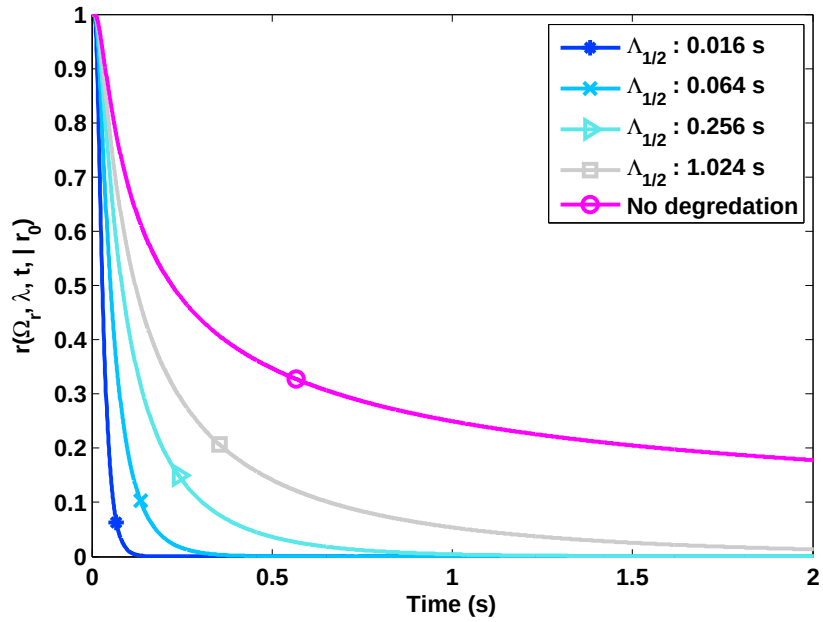

Figure 5.1. Fraction of unreceived molecules in the system for various $\Lambda_{1/2}$ values. Faster degradation shortens the tail of the unreceived molecule distribution, decreasing the amount of stray molecules and, consequently, ISI. ($d = 4\ \mu m$).

for relatively short symbol durations around $t_s = 0.2\ s$.

A second observation from Figure 5.1 is that the rate of decline in $r(\Omega_r, \lambda, t|r_0)$ reduces as larger $\Lambda_{1/2}$ -smaller λ- values are selected. This reduction is the result of the terms inside the error functions in (5.2), where λ is the coefficient on t.

5.2. Molecules Left For Upcoming Symbol Durations

The communication in CvD systems is primarily impaired due to the high ISI, which is the result of arrival of stray molecules left from previous symbol durations. Addition of messenger molecule degradation to the system works as a cleaning mechanism, which reduces the amount of residual messenger molecules left from the past symbol durations.

In Figure 5.2, the fraction of molecules received in each symbol duration for four symbol durations is given at $t_s = 60\ msec$. The figure reads, for the system with no molecular decomposition, the number of messenger molecules that arrive in the first

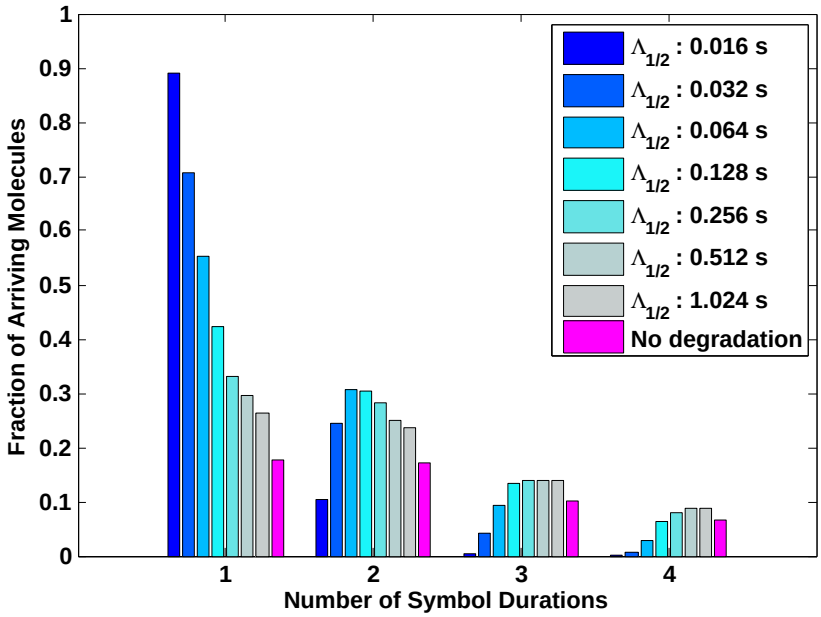

Figure 5.2. Fraction of arriving molecules for following symbol durations after a release. For higher rates of degradation, ISI in the system is significantly smaller compared to lower rate or no degradation systems.

symbol duration is approximately the same as the number of messenger molecules that arrive in the second symbol duration after the release. However, it is clear that with degradation, the difference in the number of molecules between the consecutive symbol durations increases as higher rates of degradation are utilized. Notice that for systems with $\Lambda_{1/2} = 0.016\ s$, the number of messenger molecules that arrive in the first symbol duration is nearly 9 times greater than the number of messenger molecules arrive in the second symbol duration.

5.3. Effect of Degradation on Detection Performance

For a reliable communication system, we prefer to operate with high probabilities of correct detection at the receiver side. In Figures 5.3 and 5.4, we present two ROC-curves with symbol durations equal to 0.03 and 0.04 seconds, respectively. In a binary molecular channel with thresholding, we always observe a compromise between probability of false alarm (P_f) and probability of correct detection (P_d). This is easily explained if one thinks about varying threshold mechanism used for modulation. If the detection threshold is lowered, it is always possible to achieve higher detection perfor-

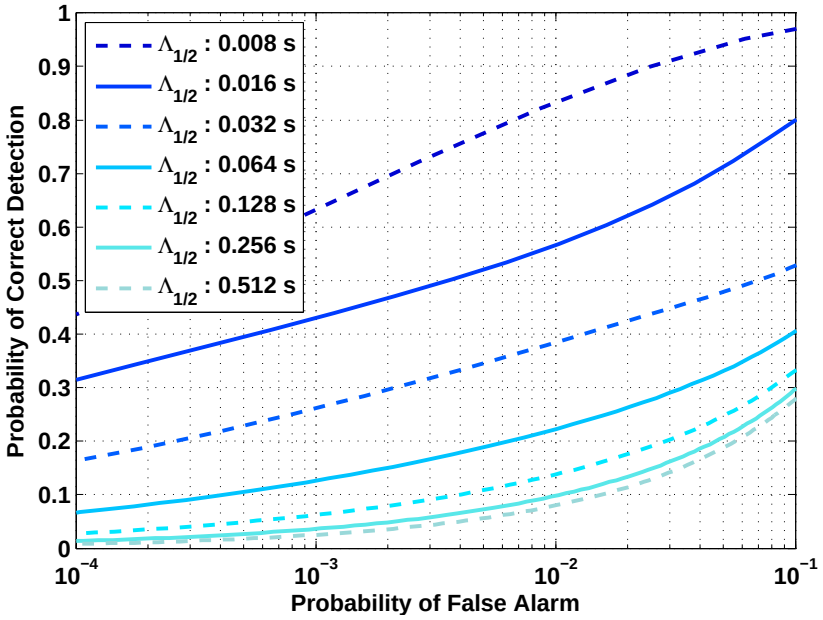

Figure 5.3. ROC curve at $t_s = 30\ msec$.

mance of a symbol-1. However, reducing τ may result in the incorrect demodulation of symbol-0 since stray molecules from previous symbol durations continue to arrive at the receiver, which in turn increases P_f.

From both Figure 5.3 and Figure 5.4, we observe a negative correlation between molecular half-life and correct detection performance. Both of the cases show clear improvements on P_d with respect to a P_f value as the molecular half-lives decrease. This indicates degradation of messenger molecules reduces the amount of stray molecules causing ISI in the receiver and increases detection performance in the molecular channel.

Comparing Figure 5.3 and 5.4, we deduce that increased symbol duration also has a positive effect on the ROC-curve. When the symbol duration is longer, all cases with different half-lives show increased performance, where the improvement on $\Lambda_{1/2} = 0.016\ s$ case is larger than $\Lambda_{1/2} = 0.008\ s$ case. This is also consistently observed in Figure 5.5, where $\Lambda_{1/2} = 0.016\ s$ results in more improvement between symbol durations [0.03, 0.04] and consequently has a larger slope. The reason behind this difference lies within the difference between the two channels' potential for improvement for the selected range of symbol durations. Both channels show very little improvement

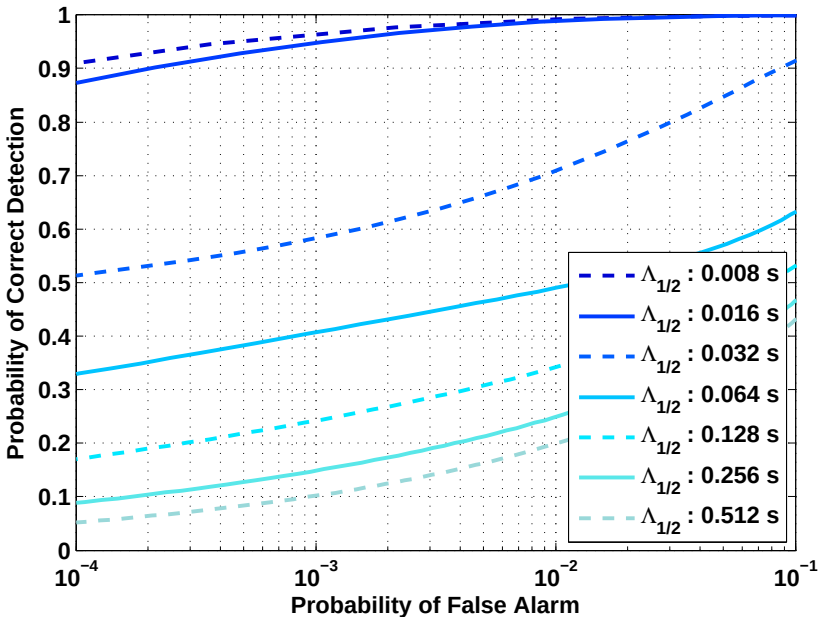

Figure 5.4. ROC curve at $t_s = 40\ msec$.

on Pe_0 values since most of the stray molecules are cleared with each case of degradation speed. This leaves improvement in Pe_1 as the reason for the difference in the potential, where $\Lambda_{1/2} = 0.008\ s$ shows a very small amount of improvement whilst $\Lambda_{1/2} = 0.016\ s$ displays a larger one. This potential difference comes from the amount of molecules staying in the system as stray molecules. One can observe, when symbol duration is larger, these molecules are no longer stray molecules but sources of information transfer to the receiver and result in a reduction in Pe_1. To conclude, while destroying molecules improves ISI, it also reduces the amount of information transferred to the receiver side, limiting the potential for improvement in the system. This limitation causes significant increase in Pe_1 when we select too small half-lives in system.

5.4. Effect of Degradation on Bit Error Rate

In order to observe the effect of the molecular degradation on the error rate in system, we look at bit error rate (BER) metric, defined as the minimum total probability of error given fixed symbol duration, number of molecules, and half-life:

$$BER = Pe = \min_{\tau} \left[Pe_0(N, \tau, \lambda) + Pe_1(N, \tau, \lambda) \right]. \tag{5.3}$$

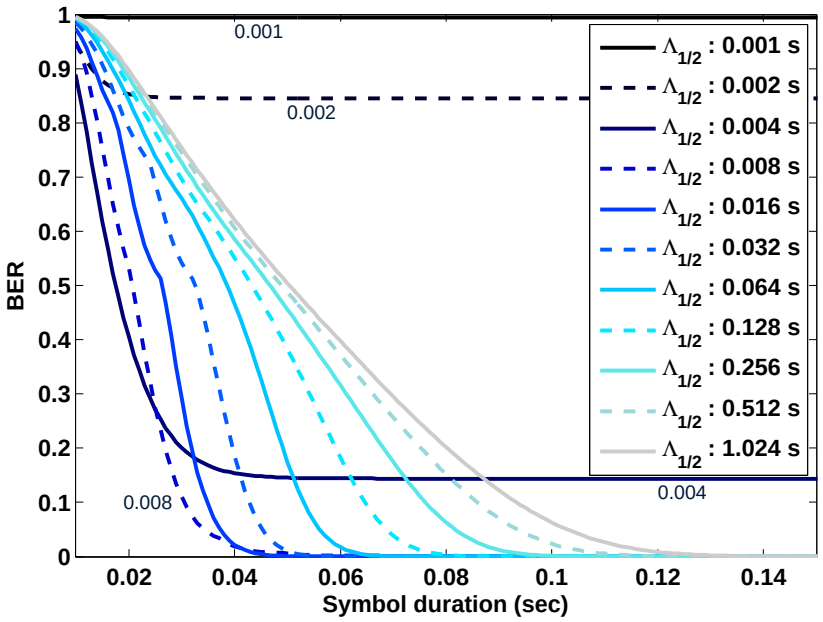

Figure 5.5. BER for various $\Lambda_{1/2}$ values. The rate of decrease in BER increases as smaller half-lives are utilized. Channels with too small half-lives, however, suffer from increased Pe_1, which lower bounds the BER over 0-level. ($d = 4\ \mu m$)

In Figure 5.5, we display the change in BER for various half-life values as the selected symbol duration increases. One can observe from the figure that down to $\Lambda_{1/2} = 0.008\ s$ increase in degradation speed increases the rate of decrease of BER as larger symbol durations are selected. This allows selecting smaller symbol durations without any performance impairment. On the other hand, selecting smaller half-lives than $0.008s$ results in a BER that has a lower bound caused by the contribution of Pe_1. At faster degradation rates, Pe_0 is the larger contributor to the overall error, since molecular communication systems suffer from ISI significantly. However, at smaller rates, molecules get destroyed so fast that they cannot deliver the encoded information to the receiver. In Figure 5.5, we observe $\Lambda_{1/2} = 0.004\ s$ has a better BER than $\Lambda_{1/2} = 0.008\ s$ for shorter symbol durations. However, as the symbol durations get longer, BER of $\Lambda_{1/2} = 0.004\ s$ gets lower bounded and is outperformed by $\Lambda_{1/2} = 0.008\ s$. Same condition is also observed for $\Lambda_{1/2} = 0.002\ s$ and $\Lambda_{1/2} = 0.001\ s$ where they are outperformed much more quickly as they impair correct detection performance more significantly.

5.5. Effect of Degradation on Data Rate

Data rate is a chief indicator of the performance of a communication system. In this section, we elaborate on the effects of degradation on the expected data rate (EDR), simply calculated as

$$\text{EDR} \quad = \quad (1 - Pe)/t_s. \tag{5.4}$$

The outcomes of selecting different degradation rates subject to different symbol durations and communication distances will be demonstrated in the following subsections.

5.5.1. Symbol Duration Selection

In Section 5.4, we observed that we can select shorter symbol durations without causing significant increase in Pe when we utilize molecular degradation in a communication via diffusion system. In this section, we elaborate on the selection of the symbol duration length to achieve the best data rate.

In Figure 5.5, we observe that faster degradation enables the increase of the data rate by providing a wider range of symbol durations in which Pe is low. Therefore, in Figure 5.6 the peak data rates are at shorter symbol durations for faster degrading molecules, excluding $\Lambda_{1/2} = 0.001,\ 0.002,\ 0.004\ s$. Consistent with Figure 5.5, $\Lambda_{1/2} = 0.001\ s$ and $\Lambda_{1/2} = 0.002\ s$ systems remain at lower data rates as their BER has error floor due to Pe_1. The case of $\Lambda_{1/2} = 0.004\ s$ in particular needs elaboration. Even though the BER for $\Lambda_{1/2} = 0.004\ s$ has error floor over zero, it manages to match the highest data rate for a shorter symbol duration. Moreover, after the optimal t_s, its data rate continues to remain below the others because of the error floor on Pe while all slower degradation cases converge to the same tail.

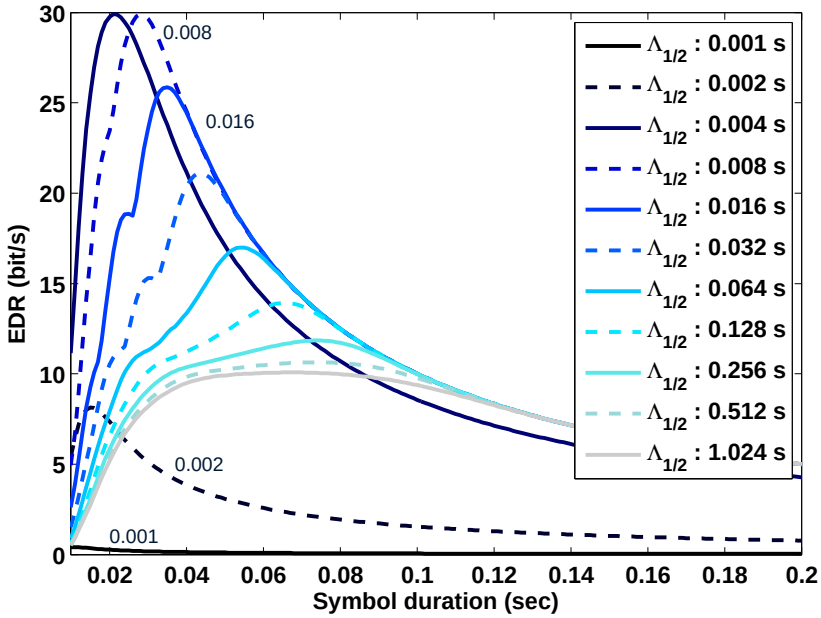

Figure 5.6. Achievable data rates for various half-lives. Reducing degradation half-life until $\Lambda_{1/2} = 0.004\ s$ increases the data rate due to the reduced ISI. However, shorter degradation half-lives increase the BER and lower the data rate in general. $(d = 4\ \mu m)$

5.5.2. Distance Selection

Degradation results in different behavior regarding channel performance for various distances. Shortening of the time required to travel to the receiver allows the utilization of faster degradation, which in turn increases the achievable data rate in the system. On the other hand, for longer distances the travel time is much larger and degradation may result in the destruction of all molecules and reduce the achievable data rate.

In Figure 5.7, we present the maximum data rate achievable with the optimal symbol duration for different distances. From the figure we first observe significant increases in data rate with the utilization of degradation for all distances. On smaller distances, best data rate is achieved with faster degradation speeds (i.e. $\Lambda_{1/2} = 0.0005\ s$) which clears the channel from the stray molecules better than the slower ones. However, on longer distances, due to the travel time required, these fast degradation systems fail to achieve higher data rates. Instead, they perform even worse than slower and no

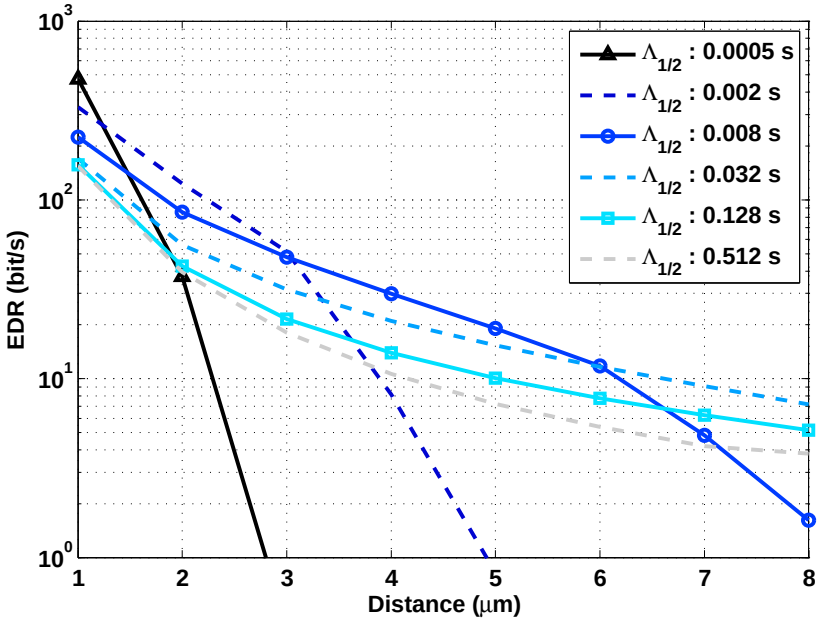

Figure 5.7. The change in data rate with different distances at various degradation rates. For small distances fast degradation rates significantly improve the data rate ($\times 3$ for $d = 1\ \mu m$ at $\Lambda_{1/2} = 0.0005\ s$). However, as the communication distance gets larger fast degradation increases Pe and significantly decreases data rate.

degradation ones because of their increased Pe_1.

6. CONCLUSION

Molecular communication via diffusion is a promising system, envisioned to be the enabler of many nanonetworking scenarios. To improve MCvD modeling, in this thesis, we elaborate on more accurate receiver modeling and incorporation of messenger molecule degradation to the MCvD system. The main contributions of this thesis are detailed below:

- *Channel characteristics for the absorbing receiver*: For the first time in the nanonetworking literature, we analytically formulate and infer channel behavior based on channel characteristics. In the thesis, the pulse peak time and the pulse peak amplitude are analyzed to gain insight on the molecular channel. The pulse peak time (relating to the speed of the signal in the channel) is found as

$$t_{peak} = d^2/6D,$$

  only depending on the communication distance and the diffusion coefficient. From this, we infer the signal propagation time is correlated to the square of the distance as oppose to the linear correlation found in EM systems.
- *Channel response for the exponential degradation*: Receiver modeling is an important part of MCvD modeling. The nanonetworking literature only focuses on concentration based or 1-D receiver models, which only provide limited accuracy. In this thesis, we develop an analytical 3-D model as an absorbing sphere under messenger molecule degradation. The channel response for this receiver is found as

$$h(\Omega_r, \lambda, t|r_0) = \frac{r_r}{r_0}\frac{1}{\sqrt{4\pi Dt}}\frac{r_0 - r_r}{t}\exp\left[-\frac{(r_0 - r_r)^2}{4Dt} - \lambda t\right], \tag{6.1}$$

and the fraction of received molecules is found as

$$\begin{aligned} w(\Omega_r, \lambda, t|r_0) &= \frac{r_r}{r_0} e^{-\sqrt{\frac{\lambda}{D}}(r_0 - r_r)} - \frac{r_r}{2r_0} \cdot e^{-\sqrt{\frac{\lambda}{D}}(r_0 - r_r)} \\ &\times \left\{ \text{erf}\left(\frac{r_0 - r_r}{\sqrt{4Dt}} - \sqrt{\lambda t} \right) + e^{2\sqrt{\frac{\lambda}{D}}(r_0 - r_r)} \right. \\ &\times \left. \left[\text{erf}\left(\frac{r_0 - r_r}{\sqrt{4Dt}} + \sqrt{\lambda t} \right) - 1 \right] + 1 \right\}. \end{aligned} \tag{6.2}$$

This formulation enables further studies to be conducted using a closed formula of an accurate receiver model.

- *Channel characteristics for the exponential degradation*: Using the channel response formula derived previously, we construct the analytic solutions to the channel characteristics of the degradation channel. These characteristics indicate that the signal propagation time (i.e. pulse peak time) now has a linear correlation with the communication distance. However, in the degradation scenario we also observe a much larger channel attenuation, correlated to $1/d^{3/2}e^{d}$ as opposed to the no degradation case where the attenuation is correlated to $1/d^{3}$.
- *Performance evaluation of the use of messenger molecule degradation in molecular communication*: The last contribution of this thesis is concentrated on the performance analysis of a degradation system. The results indicate that right amount of degradation contributes to an increase in the system performance up to three times compared to the base case of no degradation in the EDR metric. The degradation is observed to notably increase the detection performance and reduce the bit error rate in the system. Along with positive effects of degradation, we can conclude that using too fast degradation causes performance deterioration since arrival of messenger molecules becomes too sparse for the information to be transferred.

REFERENCES

1. Freitas, R. A., *Nanomedicine, Volume I: Basic Capabilities*, Landes Bioscience, Georgetown, TX, 1999.

2. Bath, J. and A. J. Turberfield, "DNA Nanomachines", *Nature nanotechnology*, Vol. 2, No. 5, pp. 275–284, 2007.

3. Singh, R. and J. W. Lillard Jr, "Nanoparticle-based Targeted Drug Delivery", *Experimental and molecular pathology*, Vol. 86, No. 3, pp. 215–223, 2009.

4. Modi, S., M. Swetha, D. Goswami, G. D. Gupta, S. Mayor, and Y. Krishnan, "A DNA Nanomachine That Maps Spatial and Temporal pH Changes Inside Living Cells", *Nature Nanotechnology*, Vol. 4, No. 5, pp. 325–330, 2009.

5. Jornet, J. M. and I. F. Akyildiz, "Graphene-based Nano-antennas for Electromagnetic Nanocommunications in the Terahertz Band", *Antennas and Propagation (EuCAP), 2010 Proceedings of the Fourth European Conference on*, pp. 1–5, IEEE, 2010.

6. Jornet, J. M. and I. F. Akyildiz, "Channel Modeling and Capacity Analysis for Electromagnetic Wireless Nanonetworks in the Terahertz Band", *Wireless Communications, IEEE Transactions on*, Vol. 10, No. 10, pp. 3211–3221, 2011.

7. Kuscu, M. and O. B. Akan, "A Nanoscale Communication Channel with Fluorescence Resonance Energy Transfer (FRET)", *Computer Communications Workshops (INFOCOM WKSHPS), 2011 IEEE Conference on*, pp. 425–430, IEEE, 2011.

8. Kuscu, M. and O. B. Akan, "A Physical Channel Model and Analysis for Nanoscale Molecular Communications with Förster Resonance Energy Transfer (FRET)", *Nanotechnology, IEEE Transactions on*, Vol. 11, No. 1, pp. 200–207, 2012.

9. Kuscu, M. and O. B. Akan, "Multi-Step FRET-Based Long-Range Nanoscale Communication Channel", *Selected Areas in Communications, IEEE Journal on*, Vol. 31, No. 12, pp. 715–725, 2013.

10. Kuscu, M. and O. B. Akan, "Coverage and Throughput Analysis for FRET-based Mobile Molecular Sensor/actor Nanonetworks", *Nano Communication Networks*, 2014.

11. Kosuta, S., S. Hazledine, J. Sun, H. Miwa, R. J. Morris, J. A. Downie, and G. E. Oldroyd, "Differential and Chaotic Calcium Signatures in the Symbiosis Signaling Pathway of Legumes", *Proceedings of the National Academy of Sciences*, Vol. 105, No. 28, pp. 9823–9828, 2008.

12. Höfer, T., L. Venance, and C. Giaume, "Control and Plasticity of Intercellular Calcium Waves in Astrocytes: A Modeling Approach", *The Journal of neuroscience*, Vol. 22, No. 12, pp. 4850–4859, 2002.

13. Kuran, M. S., T. Tugcu, and B. Ozerman, "Calcium Signaling: Overview and Research Directions of a Molecular Communication Paradigm", *Wireless Communications, IEEE*, Vol. 19, No. 5, pp. 20–27, 2012.

14. Nakano, T. and J.-Q. Liu, "Design and Analysis of Molecular Relay Channels: An Information Theoretic Approach", *NanoBioscience, IEEE Transactions on*, Vol. 9, No. 3, pp. 213–221, 2010.

15. Scemes, E. and C. Giaume, "Astrocyte Calcium Waves: What They are and What They Do", *Glia*, Vol. 54, No. 7, pp. 716–725, 2006.

16. Moore, M., A. Enomoto, T. Nakano, R. Egashira, T. Suda, A. Kayasuga, H. Kojima, H. Sakakibara, and K. Oiwa, "A Design of a Molecular Communication System for Nanomachines Using Molecular Motors", *Pervasive Computing and Communications Workshops, 2006. PerCom Workshops 2006. Fourth Annual IEEE International Conference on*, pp. 6–pp, IEEE, 2006.

17. Agarwal, A., *Engineering Applications of Kinesin Motor Proteins and Microtubule Filaments*, Ph.D. thesis, University of Florida, 2009.

18. Hess, H. and V. Vogel, "Molecular Shuttles Based on Motor Proteins: Active Transport in Synthetic Environments", *Reviews in Molecular Biotechnology*, Vol. 82, No. 1, pp. 67–85, 2001.

19. Parcerisa Giné, L. and I. F. Akyildiz, "Molecular Communication Options for Long Range Nanonetworks", *Computer Networks*, Vol. 53, No. 16, pp. 2753–2766, 2009.

20. Purnamadjaja, A. H. and R. A. Russell, "Bi-directional Pheromone Communication Between Robots", *Robotica*, Vol. 28, No. 1, pp. 69–79, 2010.

21. Cooper, G. M. and R. E. Hausman, *The Cell*, Sinauer Associates Sunderland, 2000.

22. Friedmann, T. and R. Roblin, "Gene Therapy for Human Genetic Disease?", *Science*, Vol. 175, No. 4025, pp. 949–955, 1972.

23. Huang, S. and M. Kamihira, "Development of Hybrid Viral Vectors for Gene Therapy", *Biotechnology advances*, Vol. 31, No. 2, pp. 208–223, 2013.

24. Gossler, A., T. Doetschman, R. Korn, E. Serfling, and R. Kemler, "Transgenesis by Means of Blastocyst-derived Embryonic Stem Cell Lines", *Proceedings of the National Academy of Sciences*, Vol. 83, No. 23, pp. 9065–9069, 1986.

25. Zemelman, B. V., G. A. Lee, M. Ng, and G. Miesenböck, "Selective Photostimulation of Genetically chARGed Neurons", *Neuron*, Vol. 33, No. 1, pp. 15–22, 2002.

26. Zemelman, B. V., N. Nesnas, G. A. Lee, and G. Miesenböck, "Photochemical Gating of Heterologous Ion Channels: Remote Control Over Genetically Designated Populations of Neurons", *Proceedings of the National Academy of Sciences*, Vol. 100, No. 3, pp. 1352–1357, 2003.

27. Lima, S. Q. and G. Miesenböck, "Remote Control of Behavior Through Genetically

Targeted Photostimulation of Neurons", *Cell*, Vol. 121, No. 1, pp. 141–152, 2005.

28. Claridge-Chang, A., R. D. Roorda, E. Vrontou, L. Sjulson, H. Li, J. Hirsh, and G. Miesenböck, "Writing Memories with Light-addressable Reinforcement Circuitry", *Cell*, Vol. 139, No. 2, pp. 405–415, 2009.

29. Novotny, M., "Pheromones, Binding Proteins and Receptor Responses in Rodents", *Biochemical Society Transactions*, Vol. 31, No. 1, pp. 117–122, 2003.

30. Goodman, L. S. *et al.*, *Goodman and Gilman's the Pharmacological Basis of Therapeutics*, Vol. 1157, Pergamon Press New York, 2006.

31. Tai, K., S. D. Bond, H. R. MacMillan, N. A. Baker, M. J. Holst, and J. A. McCammon, "Finite Element Simulations of Acetylcholine Diffusion in Neuromuscular junctions", *Biophysical journal*, Vol. 84, No. 4, pp. 2234–2241, 2003.

32. Bignami, G., N. Rosić, H. Michałek, M. Milošević, and G. Gatti, "Behavioral Toxicity of Anticholinesterase Agents: Methodological, Neurochemical, and Neuropsychological Aspects", *Behavioral toxicology*, pp. 155–215, Springer, 1975.

33. Srinivas, K., A. W. Eckford, and R. S. Adve, "Molecular Communication in Fluid Media: The Additive Inverse Gaussian Noise Channel", *Information Theory, IEEE Transactions on*, Vol. 58, No. 7, pp. 4678–4692, 2012.

34. Arifler, D., "Capacity Analysis of a Diffusion-based Short-range Molecular Nanocommunication Channel", *Computer Networks*, Vol. 55, No. 6, pp. 1426–1434, 2011.

35. Kuran, M. S., H. B. Yilmaz, T. Tugcu, and I. F. Akyildiz, "Modulation Techniques for Communication via Diffusion in Nanonetworks", *Communications (ICC), 2011 IEEE International Conference on*, pp. 1–5, IEEE, 2011.

36. Chou, C. T., "Molecular Circuits for Decoding Frequency Coded Signals in Nanocommunication Networks", *Nano Communication Networks*, Vol. 3, No. 1, pp.

46–56, 2012.

37. Yilmaz, H. B., N.-R. Kim, and C.-B. Chae, "Effect of ISI Mitigation on Modulation Techniques in Communication via Diffusion", *arXiv preprint arXiv:1401.3410*, 2014.

38. Bird, R. B., W. E. Stewart, and E. N. Lightfoot, *Transport Phenomena*, Wiley, Hoboken, NJ, 2006.

39. Moore, M. J. and T. Nakano, "Synchronization of Inhibitory Molecular Spike Oscillators", *Bio-Inspired Models of Networks, Information, and Computing Systems*, pp. 183–195, Springer, 2012.

40. Mahfuz, M. U., D. Makrakis, and H. T. Mouftah, "Strength-based Optimum Signal Detection in Concentration-encoded Pulse-transmitted OOK Molecular Communication with Stochastic Ligand-receptor Binding", *Simulation Modelling Practice and Theory*, 2013.

41. Pierobon, M. and I. F. Akyildiz, "Capacity of a Diffusion-based Molecular Communication System with Channel Memory and Molecular Noise", 2013.

42. Kilinc, D. and O. B. Akan, "Receiver Design for Molecular Communication", *Selected Areas in Communications, IEEE Journal on*, Vol. 31, No. 12, pp. 705–714, 2013.

43. Stirzaker, D., "Stochastic Processes and Models", *OUP Catalogue*, 2005.

44. Nakano, T., Y. Okaie, and J.-Q. Liu, "Channel Model and Capacity Analysis of Molecular Communication with Brownian Motion", *Communications Letters, IEEE*, Vol. 16, No. 6, pp. 797–800, 2012.

45. Hiyama, S. and Y. Moritani, "Molecular Communication: Harnessing Biochemical Materials to Engineer Biomimetic Communication Systems", *Nano Communication Networks*, Vol. 1, No. 1, pp. 20–30, 2010.

46. Noel, A., K. C. Cheung, and R. Schober, "Using Dimensional Analysis to Assess Scalability and Accuracy in Molecular Communication", *Communications Workshops (ICC), 2013 IEEE International Conference on*, pp. 818–823, IEEE, 2013.

47. Kuran, M. S., H. B. Yilmaz, T. Tugcu, and B. Özerman, "Energy Model for Communication via Diffusion in Nanonetworks", *Nano Communication Networks*, Vol. 1, No. 2, pp. 86–95, 2010.

48. Kuran, M. S., H. B. Yilmaz, T. Tugcu, and I. F. Akyildiz, "Interference Effects on Modulation Techniques in Diffusion Based Nanonetworks", *Nano Communication Networks*, Vol. 3, No. 1, pp. 65–73, 2012.

49. Kuran, M. S., H. B. Yilmaz, and T. Tugcu, "A Tunnel-based Approach for Signal Shaping in Molecular Communication", *Communications Workshops (ICC), 2013 IEEE International Conference on*, pp. 776–781, IEEE, 2013.

50. Akkaya, A. and T. Tugcu, "dMCS: Distributed Molecular Communication Simulator", *Proceedings of the 8th International Conference on Body Area Networks*, pp. 468–471, ICST (Institute for Computer Sciences, Social-Informatics and Telecommunications Engineering), 2013.

51. Liu, Q. and K. Yang, "Channel Capacity Analysis of a Diffusion-based Molecular Communication System with Ligand Receptors", *International Journal of Communication Systems*, 2014.

52. Noel, A., K. C. Cheung, and R. Schober, "Improving Diffusion-based Molecular Communication With Unanchored Enzymes", *arXiv preprint arXiv:1305.1783*, 2013.

53. Tyrrell, H. J. V. and K. Harris, *Diffusion in Liquids, A Theoretical and Experimental Study*, Butterworth Publishers, Stoneham, MA, 1984.

54. Redner, S., *A Guide to First-passage Processes*, Cambridge University Press, Cam-

bridge UK, 2001.

55. Schulten, K. and I. Kosztin, "Lectures in Theoretical Biophysics", *University of Illinois*, Vol. 117, 2000.

56. Philippidis, G. P., T. K. Smith, and C. E. Wyman, "Study of the Enzymatic Hydrolysis of Cellulose for Production of Fuel Ethanol by the Simultaneous Saccharification and Fermentation Process", *Biotechnology and bioengineering*, Vol. 41, No. 9, pp. 846–853, 1993.

57. Phillips, J., "Stretched Exponential Relaxation in Molecular and Electronic Glasses", *Reports on Progress in Physics*, Vol. 59, No. 9, p. 1133, 1996.

58. Berg, H. C., *Random Walks in Biology*, Princeton University Press, Princeton, N.J., 1993.

59. Butler, K. and M. Stephens, "The Distribution of a Sum of Binomial Random Variables", Technical report, DTIC Document, 1993.